Revised and expanded 30 Dec 1996
FTUAM 96-39
hep-ph/96 10380

Theory of Small x Deep Inelastic Scattering : NLO Evaluations, and low Q^2 Analysis*

K. Adel,
F. Barreiro
and
F. J. Yndurain**

Departamento de Física Teórica, C-XI
Universidad Autónoma de Madrid
Canto Blanco, 28049-Madrid

ABSTRACT.

We calculate structure functions at small x both under the assumption of a hard singularity (essentially, a power behaviour $x^{-\lambda}$, λ positive, for $x \to 0$) or that of a soft-Pomeron dominated behaviour, also called double scaling limit, for the singlet component. A full next to leading order (NLO) analysis is carried for the functions F_2, $F_{\rm Glue}$ and the longitudinal one F_L in ep scattering, and for xF_3 in neutrino scattering. The results of the calculations are compared with experimental data, particularly the recent ones from HERA, in the range $x \leq 0.032$, $10\ {\rm GeV}^2 \leq Q^2 \leq 1\,500\ {\rm GeV}^2$. We get reasonable fits, with a chi-squared/d.o.f. around two unities, with only three-four parameters for both assumptions, but none of the assumptions is by itself able to give a fully satisfactory description of the data. The results improve substantially if *combining* a soft and a hard component; in this case it is even possible to extend the analysis, phenomenologically, to small values of Q^2, $0.31\,{\rm GeV}^2 \leq Q^2 \leq 8.5\,{\rm GeV}^2$, and in the x range $6 \times 10^{-6} \lesssim x \lesssim 0.04$, with the same hard plus soft Pomeron hypothesis by assuming a saturating expression for the strong coupling,

$$\tilde{\alpha}_s(Q^2) = 4\pi/\beta_0 \log[(Q^2 + \Lambda^2_{\rm eff})/\Lambda^2_{\rm eff}].$$

The description for low Q^2 implies self-consistent values for the parameters in the exponents of x both for singlet and nonsinglet components. One has to have, for the Regge intercepts, $\alpha_\rho(0) = 0.48$ and $\alpha_P(0) = 1.470$ [$\lambda = 0.470$], in uncanny agreement with other determinations of these parameters, and in particular the results of the large Q^2 fits. The fit to data is so good that we may look (at large Q^2) for signals of a "triple Pomeron" vertex, for which some evidence is found.

The quality of the calculations of F_2, and of the predictions for $F_{\rm Glue}$, F_L is only marred by the *very* large size of the NLO corrections for the singlet part of F_2. This, in particular, forbids a truly reliable determination of the QCD parameter, Λ.

* This paper includes the results from FTUAM 96-39 [hep-ph 96 10380] and FTUAM 96-44 [hep-ph 96 12469]

** e-mail: fjy@delta.ft.uam.es

-Adel, Barreiro and Ynduráin-

1. INTRODUCTION

In two recent papers[1,2] it was shown how the recent HERA data[3,4] on electroproduction at small x could be very well fitted by the formulas, proposed long ago by C. López and one of us[5,6] which to leading order (LO) read,

$$F_2(x,Q^2) = \langle e_q^2\rangle [F_S(x,Q^2) + F_{NS}(x,Q^2)], \tag{1.1a}$$

$$F_S(x,Q^2) \underset{x\to 0}{\simeq} B_S\, \alpha_s^{-d_+} x^{-\lambda}, \tag{1.1b}$$

$$F_{NS}(x,Q^2) \underset{x\to 0}{\simeq} B_{NS}\, \alpha_s^{-d_{NS}} x^{\rho},\ \rho \sim 0.5. \tag{1.2}$$

Here d_+ and d_{NS} are known quantities related to the singlet anomalous dimension matrix $\mathbf{D}$ and to the nonsinglet anomalous dimension; B_S, B_{NS}, λ are free parameters. In ref. 2, the analysis was extended to the gluon structure function, while the longitudinal one (to LO) had been considered in ref. 8. One has,

$$F_G(x,Q^2) \underset{x\to 0}{\simeq} B_G \alpha_s^{-d_+} x^{-\lambda}, \tag{1.3a}$$

and

$$R \equiv F_L/F_2 \underset{x\to 0}{\simeq} r_0 \frac{\alpha_s}{\pi} = \frac{C_F \alpha_s}{\pi(2+\lambda)} \left\{ 1 + \frac{4T_F n_f}{(3+\lambda)C_F} \frac{B_G}{B_S} \right\}, \tag{1.3b}$$

with $B_G/B_S = (d_+ - D_{11})/D_{12}$. These formulas follow at leading order from perturbative QCD, plus the assumption that the leading singularity in n of the matrix elements (for e.g. the singlet case)

$$\langle p|\mathbf{a}_n|p\rangle;\ \mathbf{a}_n = \begin{pmatrix} \bar{q}_f \gamma \overbrace{\partial \ldots \partial}^{n-1} q_f \\ G \underbrace{\partial \ldots \partial}_{n-2} G \end{pmatrix}$$

are located to the right of those of the corresponding anomalous dimensions, $\mathbf{D}$, d_{NS} (For more details, see refs. 1, 5, 6, 7).

An alternate possibility, that may be called "soft-Pomeron" dominated, occurs when the singularity of $\mathbf{D}$ is the leading one; it was proposed first by De Rújula et al.[9] The ensuing LO behaviour for the structure functions F_S, F_G was evaluated in detail by F. Martin[10] and, for R, in ref. 8. The next to leading order (NLO) corrections to F_S were given in ref. 11. To LO one has,

$$\begin{aligned} F_S &\simeq \frac{c_0}{|\log x|} \left[\frac{9|\log x| \log[\alpha_s(Q_0^2)/\alpha_s(Q^2)]}{4\pi^2(33-2n_f)} \right]^{\frac{1}{4}} \\ &\times \exp\left\{ \sqrt{d_0 |\log x| \left[\log \frac{\alpha_s(Q_0^2)}{\alpha_s(Q^2)}\right]} - d_1 \log \frac{\alpha_s(Q_0^2)}{\alpha_s(Q^2)} \right\}, \end{aligned} \tag{1.4a}$$

$$\begin{aligned} F_G &\simeq \frac{9c_0}{n_f} \left[\frac{33-2n_f}{576\pi^2 |\log x| \log[\alpha_s(Q_0^2)/\alpha_s(Q^2)]} \right]^{\frac{1}{4}} \\ &\times \exp\left\{ \sqrt{d_0 |\log x| \left[\log \frac{\alpha_s(Q_0^2)}{\alpha_s(Q^2)}\right]} - d_1 \log \frac{\alpha_s(Q_0^2)}{\alpha_s(Q^2)} \right\}, \end{aligned} \tag{1.4b}$$

$d_0 = 144/(33-2n_f)$, $d_1 = (33+2n_f/9)/(33-2n_f)$, and

$$R \simeq \left[\frac{(33-2n_f)|\log x|}{\log[\alpha_s(Q_0^2)/\alpha_s(Q^2)]} \right]^{\frac{1}{2}} \frac{\alpha_s(Q^2)}{2\pi}, \tag{1.4c}$$

to be compared with Eqs. (1.1), (1.3). We will discuss this possibility in Sect. 4.

Returning to our first case, the analysis was extended in ref. 2 to practically the whole range of HERA data at the cost of introducing phenomenological correction terms for "large" values of x, $x > 0.01$, and small $Q^2 < 12\ \mathrm{GeV}^2$. Moreover, only the LO prediction for R was evaluated. Here we go a few steps forward, in the following directions. First, we perform a full NLO analysis, including that of the longitudinal structure function. Second, we extend the analysis to incorporate the function xF_3 for neutrino scattering which provides pure nonsinglet function, hence a

combination independent from that in (1.1a): this helps stabilize the results. Then, for the hard Pomeron case, we include theoretically justified corrections, and resummations, which enable us to extend the range of validity of the formulas (as determined e.g. in ref. 1) and to paliate somewhat the effects of the hughe size of the NLO corrections to the singlet component of F_2, which are of some $\sim 6\alpha_s$.

For the soft Pomeron dominance hypothesis we again perform a full NLO calculation of F_S, F_G and F_L. NLO corrections are, also in this case, very large; their size is indeed the only serious drawback for our results, otherwise able to describe reasonably well the HERA data in a wide range, and providing believable predictions for the gluon and longitudinal structure functions. This agreement of theoretical predictions and data is essentially true both for the soft and hard Pomeron hypotheses, an apparently surprising fact that is discussed in Sect. 5. Here we argue that a possible reason is that F_S contains *both* a hard and a soft piece. In fact, we are able to give excellent fits to all HERA data ($x \leq 0.032$) by using a formula sum of (1.1) and (1.4). This provides us with the best fits to the data, the parameters of which are reported in Table X.

In Sect. 6 we show that the fit with a soft plus a hard Pomeron may be phenomenologically extended to low Q^2, down to 0.31 GeV^2, provided we make a saturation assumption for the strong coupling α_s and satisfy a self-consistency condition for the parameters λ, ρ. This fixes these parameters to the values $\lambda = 0.470$, $\rho = 0.522$, in uncanny agreement with other (in particular high Q^2, Sect. 5) determinations.

2. THEORETICAL EVALUATIONS (HARD SINGULARITY)

We will here briefly rederive the extension to NLO of the equations governing the behaviour of structure functions as $x \to 0$; not only for ease of reference, but because the large size of the *singlet* NLO corrections makes it convenient to use formulas more precise than those employed in refs. 2, 6. We will also extend the analysis to the longitudinal structure function at NLO.

2.1. Nonsinglet

Defining the moments

$$\mu_{NS}(n,Q^2) = \int_0^1 \mathrm{d}x\, x^{n-2} F_{NS}(x,Q^2), \tag{2.1}$$

they satisfy the QCD evolution equations

$$\mu_{NS}(n,Q^2) = \mathrm{e}^{-\int_{t_0}^{t} \mathrm{d}t'\, \gamma_{NS}(n,g(t'))} C_{NS}(n,\alpha_s(Q^2)), \tag{2.2}$$

where $t = \log Q^2$, g is the coupling constant, γ_{NS} the nonsinglet (NS) anomalous dimension, and C_{NS} the NS Wilson coefficient[1]. The first singularity of γ_{NS} to LO and NLO lies at $n = 0$. If we assume this to occur to all orders, and that F_{NS} behaves like a power x^ρ as x goes to zero, we get the following behaviour from (2.2):

$$F_{NS}(x,Q^2) \underset{x\to 0}{\simeq} (\mathrm{Const.})\, x^\rho\, \mathrm{e}^{-\int_{t_0}^{t} \mathrm{d}t'\, \gamma_{NS}(1-\rho,g(t'))} C_{NS}(1-\rho,\alpha_s(Q^2)). \tag{2.2}$$

Expanding γ_{NS}, g, C_{NS} to second order and integrating we get,

$$F_{NS}(x,Q^2) \underset{x\to 0}{\simeq} B_{NS}\, x^\rho \left[1 + \frac{C_{NS}^{(1)}(1-\rho)\alpha_s(Q^2)}{4\pi} + \dots\right]$$

$$\times \exp\left\{ d_{NS}(1-\rho)\log\alpha_s^{-1}(Q^2) + \frac{q_{NS}(1-\rho)\alpha_s(Q^2)}{4\pi} + \dots \right\}, \tag{2.4}$$

B_{NS} a constant and

$$d_{NS}(n) = -\gamma_{NS}^{(0)}(n)/2\beta_0$$

$$q_{NS}(n) = \frac{\beta_1 d_{NS}(n)}{\beta_0} + \frac{\gamma_{NS}^{(1)}(n)}{2\beta_0}.$$

[1] The anomalous dimensions and coefficients are collected in the Appendix for ease of reference.

The values of the quantities β_i, C_{NS}, $\gamma_{NS}^{(i)}$ may be found in refs. 6, 7. Eq. (2.4) may be conveniently rewritten (suppressing the dots) as

$$F_{NS}(x,Q^2) \underset{x\to 0}{\simeq} B_{NS}\left\{1+\frac{C_{NS}^{(1)}(1-\rho)\alpha_s(Q^2)}{4\pi}\right\} \times \mathrm{e}^{q_{NS}(1-\rho)\alpha_s/4\pi}\left[\alpha_s(Q^2)\right]^{-d_{NS}(1-\rho)} x^\rho, \tag{2.5}$$

an expression[2] in which the modifications of (1.2) due to the NLO corrections is apparent.

One can also expand the exponent in (2.5) and get

$$F_{NS}(x,Q^2) \underset{x\to 0}{\simeq} B_{NS}\left\{1+\frac{v_{NS}(1-\rho)\alpha_s(Q^2)}{4\pi}\right\}\alpha_s^{-d_{NS}} x^\rho, \tag{2.6}$$

$v_{NS} = C_{NS}^{(1)} + q_{NS}$.

For $\rho = 0.5$, a value that follows from a Regge analysis and that we will adopt here, one finds

$$v_{NS}|_{\rho=0.5, n_f=4} = 3.42, \tag{2.7}$$

so the NLO correction is small and we may use (2.5) or (2.6) indifferently.

2.2. Singlet

Eq. (2.2) is now replaced by the coupled equations

$$\boldsymbol{\mu}(n,Q^2) = (\mathrm{Const.})\mathrm{T}\ \mathrm{e}^{-\int_{t_0}^{t}\mathrm{d}t'\boldsymbol{\gamma}(n,g(t'))}\mathbf{C}(n,\alpha_s(Q^2)) \tag{2.8}$$

$$\boldsymbol{\mu}(n,Q^2) = \begin{pmatrix} \mu_S(n,Q^2) = \int_0^1 \mathrm{d}x\, x^{n-2}F_S(x,Q^2) \\ \mu_G(n,Q^2) = \int_0^1 \mathrm{d}x\, x^{n-2}F_G(x,Q^2)\end{pmatrix}.$$

Here $\boldsymbol{\gamma}$, $\mathbf{C}$ are square matrices; the operation T in (2.8) is like the familiar time ordering operator but it now orders in $t = \log Q^2$. This ordering, and the matrix character of the equations complicates the singlet analysis, the details of which may be found in refs. 6, 7. To *next* to leading order we may easily write the analogue of (2.4), (2.5) as

$$F_S(x,Q^2) \underset{x\to 0}{\simeq} B_S x^{-\lambda}\left[1+\frac{c_S(1+\lambda)\alpha_s(Q^2)}{4\pi}+\ldots\right] \times \exp\left\{d_+(1+\lambda)\log\alpha_s^{-1}(Q^2)+\frac{q_S(1+\lambda)\alpha_s(Q^2)}{4\pi}+\ldots\right\}, \tag{2.9}$$

or, suppressing the dots and in a form easier to compare with the LO expression (1.1b),

$$F_S(x,Q^2) \underset{x\to 0}{\simeq} B_S\left\{1+\frac{c_S(1+\lambda)\alpha_s(Q^2)}{4\pi}\right\} \times \mathrm{e}^{q_S(1+\lambda)\alpha_s/4\pi}\left[\alpha_s(Q^2)\right]^{-d_+(1+\lambda)} x^{-\lambda}. \tag{2.10a}$$

A corresponding equation for the gluon component we will consider later. In above equations we have

$$\mathbf{D} = -\frac{\boldsymbol{\gamma}^{(0)}}{2\beta_0},$$

$$c_S = C_{11}^{(1)} + \frac{d_+ - D_{11}}{D_{12}}C_{12}^{(1)},$$

$$q_S = \frac{\beta_1 d_+}{\beta_0} + \frac{\bar\gamma_{11}}{2\beta_0} + \frac{\bar\gamma_{21}}{2\beta_0(d_- - d_+ + 1)}\,\frac{D_{12}}{d_- - d_+},$$

$$\bar{\boldsymbol{\gamma}} = \mathbf{S}^{-1}\boldsymbol{\gamma}^{(1)}\mathbf{S},$$

and $\mathbf{S}$ is the matrix that diagonalizes $\mathbf{D}$:

$$\mathbf{S}^{-1}\mathbf{D}\mathbf{S} = \begin{pmatrix} d_+ & 0 \\ 0 & d_-\end{pmatrix}.$$

[2] Eq. (2.5) corrects the sign misprints in Eq. (2.18) of ref. 6.

One can also expand the exponential in (2.10a) and get

$$F_S(x,Q^2) \underset{x\to 0}{\simeq} B_S \left\{1+\frac{w_S(1+\lambda)\alpha_s(Q^2)}{4\pi}\right\} \alpha_s^{-d_+} x^{-\lambda}, \tag{2.10′a}$$

$w_S = c_S + q_S$. The $\bar\gamma$, q, c, w are collected in the Appendix.

Unfortunately, w_S is very large. For $\lambda = 0.35$, $n_f = 4$, $w_S = 77.8$; for $\lambda = 0.47$, $w_S = 56.7$. Therefore, we are faced with the choice of using the exponential form (2.10) or the expanded one (2.10′). The exponential form has errors of order α_s^2 because the noncommutativity of $\boldsymbol{\gamma}^{(0)}$, $\boldsymbol{\gamma}^{(1)}$ makes the T-exponential different from the ordinary exponential. If we use the expanded form (2.10′) we have other errors (also of order α_s^2) due to the large size of the neglected term $\mathrm{O}[q_S(1+\lambda)\alpha_s/4\pi]^2$. It is unclear a priori which of the two procedures will be more accurate, although the abnormally large size of $q_S(1+\lambda)$ suggests that the exponentiated form will be more precise; note that the perturbative expansion still makes sense, *for the exponent*, in that for reasonably large Q^2 one has

$$\frac{q_S\alpha_s}{4\pi} \ll d_+ \log\alpha_s^{-1}.$$

In fact, and as we will see, the exponentiated form produces somewhat more satisfactory results than the expanded one. At any rate, we will use both (2.10) and (2.10′): one may take the difference as an indication of the *theoretical* error of our calculation.

Similar considerations of course apply to the gluon component that we discuss next, although in this case the correction is much smaller ($\sim 15\alpha_s/4\pi$) so use of exponentiated or expanded form is essentially equivalent here and only consistency with the quark component will make us use one or the other. We then have,

$$\begin{aligned} F_G(x,Q^2) \underset{x\to 0}{\simeq} B_S \frac{d_+ - D_{11}}{D_{12}} \left\{1+\frac{c_G(1+\lambda)\alpha_s(Q^2)}{4\pi}\right\} \\ \times \mathrm{e}^{q_G(1+\lambda)\alpha_s/4\pi} \left[\alpha_s(Q^2)\right]^{-d_+(1+\lambda)} x^{-\lambda}, \end{aligned} \tag{2.10b}$$

where now

$$c_G = C_{11}^{(1)} + C_{12}^{(1)} \left(\frac{D_{22}-D_{11}}{D_{12}} + \frac{D_{21}}{d_+ - D_{11}}\right) \equiv c_S,$$

$$q_G = \frac{\beta_1 d_+}{\beta_0} + \frac{\bar\gamma_{11}}{2\beta_0} + \frac{\bar\gamma_{21}}{2\beta_0(d_- - d_+ + 1)} \frac{D_{12}}{d_- - d_+} \frac{d_- - D_{11}}{d_+ - D_{11}}.$$

In expanded form,

$$\begin{aligned} F_G(x,Q^2) \underset{x\to 0}{\simeq} B_S \frac{d_+ - D_{11}}{D_{12}} \left\{1+\frac{w_G(1+\lambda)\alpha_s(Q^2)}{4\pi}\right\} \left[\alpha_s(Q^2)\right]^{-d_+(1+\lambda)} x^{-\lambda}, \\ w_G(1+\lambda) \equiv c_G(1+\lambda) + q_G(1+\lambda). \end{aligned} \tag{2.10′b}$$

2.3. The longitudinal structure function

We normalize the longitudinal structure function F_L in such a way that one has

$$R(x,Q^2) = \frac{F_L}{F_S + F_{NS} - F_L}. \tag{2.11a}$$

It is also convenient to define the quantity R' by

$$R'(x,Q^2) = \frac{F_L}{F_S + F_{NS}};\ R = \frac{R'}{1-R'}. \tag{2.11b}$$

For $x \to 0$ the contribution of F_{NS} is negligible with respect to that of F_S and we will accordingly neglect it; the effect of taking it into account, to LO, may be found in ref. 8. The function F_L may be evaluated in terms of F_S, F_G. One has,

$$F_L(x,Q^2) = \int_x^1 \mathrm{d}y \left\{C_S^L(y,Q^2) F_S\left(\frac{x}{y},Q^2\right) + C_G^L(y,Q^2) F_G\left(\frac{x}{y},Q^2\right)\right\}, \tag{2.12a}$$

where the kernels C^L are,

$$\begin{aligned} C_S^L(x,Q^2) &= C_{NS}^L(x,Q^2) + C_{PS}^L(x,Q^2); \\ C_{NS}^L(x,Q^2) &= [4C_F x]\frac{\alpha_s(Q^2)}{4\pi} + c_{NS}^{(1)L}(x)\left(\frac{\alpha_s(Q^2)}{4\pi}\right)^2 + \dots \\ C_{PS}^L(x,Q^2) &= c_{PS}^{(1)L}(x)\left(\frac{\alpha_s(Q^2)}{4\pi}\right)^2 + \dots \\ C_G^L(x,Q^2) &= [16 n_f T_F x(1-x)]\frac{\alpha_s(Q^2)}{4\pi} + c_G^{(1)L}(x)\left(\frac{\alpha_s(Q^2)}{4\pi}\right)^2 + \dots . \end{aligned} \tag{2.12b}$$

The functions $c_{NS,PS,G}^{(1)L}$ are described in the Appendix[3].

Under our assumptions, Eqs. (2.10), the behaviour of F_L follows immediately; we have,

$$F_L(x,Q^2) \underset{x\to 0}{\simeq} F_S(x,Q^2)\int_0^1 \mathrm{d}x\, x^\lambda \left\{C_S^L(x,Q^2) + \eta(Q^2) C_G^L(x,Q^2)\right\}, \tag{2.13}$$

and η is the ratio

$$\eta(Q^2) = \lim_{x\to 0}\frac{F_G(x,Q^2)}{F_S(x,Q^2)}.$$

To LO a simple evaluation gives[8] $R(x,Q^2) \simeq R^{(0)}(x,Q^2)$ with

$$\begin{aligned} R^{(0)}(x,Q^2) &\underset{x\to 0}{\simeq} r_0(1+\lambda)\frac{\alpha_s}{\pi}, \\ r_0(1+\lambda) &= \frac{C_F\alpha_s}{2+\lambda}\left\{1 + \frac{4T_F n_f}{(3+\lambda)C_F}\,\frac{d_+(1+\lambda) - D_{11}(1+\lambda)}{D_{12}(1+\lambda)}\right\}. \end{aligned} \tag{2.14}$$

To NLO the calculation is made numerically. For this, define the integrals (whose values may be found in the Appendix),

$$\begin{aligned} \int_0^1 \mathrm{d}x\, x^\lambda\, c_{NS}^{(1)L}(x) &= C_F(C_A - 2C_F) I_{S1}(\lambda) + C_F^2 I_{S2}(\lambda) + C_F T_F n_f I_{S3}(\lambda), \\ \int_0^1 \mathrm{d}x\, x^\lambda\, c_{PS}^{(1)L}(x) &= C_F T_F n_f I_{PS}(\lambda), \\ \int_0^1 \mathrm{d}x\, x^\lambda\, c_G^{(1)L}(x) &= n_f T_F [C_F I_{G1}(\lambda) + C_A I_{G2}(\lambda)], \end{aligned} \tag{2.15}$$

and write, in exponentiated form,

$$\eta(Q^2) = \frac{d_+ - D_{11}}{D_{12}}\mathrm{e}^{(q_G - q_S)\alpha_s/4\pi}. \tag{2.16a}$$

Then,

$$R' = R^{(0)} + R'^{(1)} \tag{2.16b}$$

with $R^{(0)}$ as above and

$$\begin{aligned} R'^{(1)} \underset{x\to 0}{\simeq} \frac{C_F}{2+\lambda}\,\frac{\alpha_s(Q^2)}{\pi}\Bigg\{1 + \frac{2+\lambda}{4}\left[C_A I_{S1} + C_F(I_{S2} - 2I_{S1}) + n_f T_F(I_{S3} + I_{PS})\right]\frac{\alpha_s}{4\pi} \\ + \frac{4 n_f T_F}{(3+\lambda)C_F}\left[1 + \frac{(2+\lambda)(3+\lambda)}{16}(C_F I_{G1} + C_A I_{G2})\frac{\alpha_s}{4\pi}\right]\eta(Q^2)\Bigg\}. \end{aligned} \tag{2.16c}$$

3. NUMERICAL RESULTS (HARD SINGULARITY ONLY).

3.1. The function F_2.

[3] These quantities were first evaluated in refs. 12, 13. Correct values, checked at least in two independent calculations, are given in Eqs. (8), (9) of ref. 12 for $c_{NS,PS}^{(1)L}$ and in Eq. (9) of ref. 13 for $c_G^{(1)}$. The value of this quantity given in ref. 12 contains an error. The first moments of the c may be found in ref. 14; they are useful, among other things, to check the integrals (2.15) here.

LO calculations. For ease of comparison between LO and NLO evaluations we repeat here the results of a fit to the old (1993) Zeus data[3], as performed in ref. 1. The calculation is carried for 32 points in the range

$$x < 10^{-2},\ 12 \leq Q^2 \leq 90\ \mathrm{GeV}^2.$$

Because of the size of the experimental errors a LO calculation is sufficient, and the NS contribution may be neglected. The QCD parameter Λ is fixed to 0.2 GeV so that $\alpha_s(m_\tau^2) = 0.32$. The results are summarized in Table I for $n_f = 4$ flavours. The corresponding values of B_G, r_0 are also given. The agreement of the value of λ with the figure $\lambda = 0.36 \pm 0.07$ obtained in ref. 3 from data with $x \geq 0.02$, $Q^2 \leq 22\,\mathrm{GeV}^2$ is noteworthy.

Table I. "Old" Zeus data. LO. $n_f = 4; \Lambda(1\,\mathrm{loop}, n_f = 4) = 0.200\,\mathrm{GeV}; \alpha_s(m_\tau^2) = 0.32.$

λ	d_+	$\langle e_q^2\rangle B_S$	B_G/B_S	r_0	χ^2/d.o.f.
0.38 ± 0.01	2.41 ± 0.1	$(2.70 \pm 0.22) \times 10^{-3}$	20.56 ± 0.54	6.24 ± 0.24	$\frac{9.13}{32-2}$

NLO evaluation. If we only fit the H1 points[4] with $x < 10^{-2}$, $Q^2 \geq 12\ \mathrm{GeV}^2$ using the exponentiated formulas, we get a χ^2/d.o.f. is less than one, with parameters reported in Table II.

Table II. H1 plus ν data. $x \leq .01$, $n_f = 4$; $\Lambda(n_f = 4,\ 2\ \mathrm{loop})$ fixed to 0.11 GeV.

λ	$\langle e_q^2\rangle B_S$	$\langle e_q^2\rangle B_{NS}$	χ^2/d.o.f.
0.3218	1.423×10^{-4}	0.390	$\frac{48.9}{58-3}$

However, it is still not possible to give any value for the QCD parameter Λ. The reason is that the interplay between singlet and nonsinglet parts compensates the effect of varying Λ. For example, a χ^2/d.o.f. less than one is attained for $3\ \mathrm{MeV} \leq \Lambda \leq 260\,\mathrm{MeV}$. This is why we do not give errors in the parameters in Table II.

We may improve the situation as follows. First, and as discussed in ref. 1, we can include more points limited by a certain $Q^2(x)$ beyond which corrections to the leading behaviour become important. To be precise, we choose the H1 points with (Fig. 1)

$$\begin{array}{ll} Q^2 \leq 150\ \mathrm{GeV}^2, & \text{for } x = 0.013, \\ Q^2 \leq 90\ \mathrm{GeV}^2, & \text{for } x = 0.02, \\ Q^2 \leq 60\ \mathrm{GeV}^2, & \text{for } x = 0.032, \end{array} \qquad (3.1)$$

with a total of 77 points. Secondly, we incorporate small x data (a total of 10 points) from the *neutrino* structure function[15] xF_3 which is pure nonsinglet and hence provides the independent measurement necessary to disentangle the singlet and nonsinglet components of F_2: this, as we will see, gives stability to the results.

The outcome of the fits is given in Tables III, IV with Λ a free parameter. The χ^2/d.o.f. is reasonable, although its increase beyond unity reflects the fact that the subleading effects are substantial for the points $x = 0.013 \sim 0.032$.

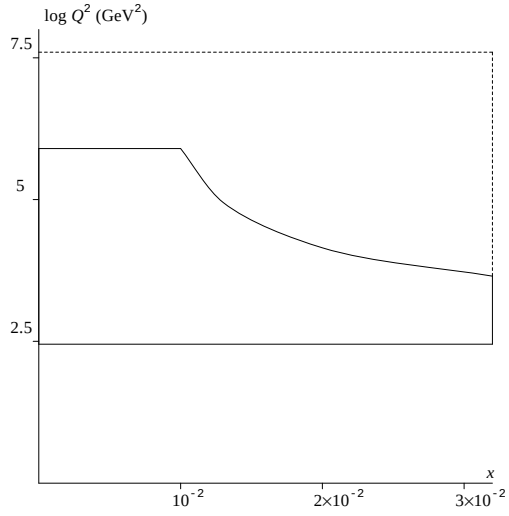

Figure 1. Area described by (3.1), bounded by a continuous line. Broken line: extended region for fit with (3.2).

Table III. H1 plus ν data; x given by (3.1). $n_f = 4$, two loops.

Λ	λ	$\langle e_q^2\rangle B_S$	$\langle e_q^2\rangle B_{NS}$	χ^2/d.o.f.
$0.080^{+0.060}_{-0.035}\,\mathrm{GeV}$	0.3243 ± 0.0065	$1.321^{+0.630}_{-0.427} \times 10^{-4}$	$0.254^{+0.025}_{-0.020}$	$\frac{97.5}{87-4}$

Table IV. H1 plus ν data; x given by (3.1). $n_f = 5$, two loops.

$\Lambda(n_f = 4,\ 2\ \mathrm{loops})$	λ	$\langle e_q^2\rangle B_S$	$\langle e_q^2\rangle B_{NS}$	χ^2/d.o.f.
$0.11^{+0.06}_{-0.05}\,\mathrm{GeV}$	0.331 ± 0.006	$1.118^{+0.444}_{-0.409} \times 10^{-4}$	$0.311^{+0.024}_{-0.072}$	$\frac{103.0}{87-4}$

From these results it is clear that the data do not discriminate between $n_f = 4,\ 5$, although the first value is slightly favoured. For this reason we will give almost exclusively fits with $n_f = 4$.

The values of Λ we obtain are compatible with standard ones[16], albeit on the small side. Because the parameters are very strongly correlated the errors given are obtained *not* by varying the parameters independently, but by varying only Λ and treating the other parameters as dependent quantities. It is also important to realize that the errors in Tables III, IV and indeed in practically all the evaluations, are purely *nominal* in the sense that we have not taken into account *theoretical* errors, which are much larger. In fact, the central values for the parameters, especially B_S, λ, depend very strongly on the theoretical assumptions[4] made; for example, they vary way beyond the nominal errors from LO to NLO: compare e.g. Table I with Table II.

The results reported in Tables III, IV were obtained with the exponentiated formula. If we use the expanded one, Eq. (2.10′a) we find the results of Table IV′.

Table IV′. H1 plus ν data; x given by (3.1). $n_f = 4$; $\Lambda(n_f = 4,\ 2\ \mathrm{loops}) = 0.080\,\mathrm{GeV}$.

λ	$\langle e_q^2\rangle B_S$	$\langle e_q^2\rangle B_{NS}$	χ^2/d.o.f.
0.3408	2.54×10^{-4}	0.268	$\frac{99.5}{87-4}$

We do not give errors, but the results of the fit for a representative value of Λ: that for which the fit with the *exponentiated* formula is optimum. This is because there is no optimum reasonable value of Λ if using the nonexponentiated expression; the χ^2 decreases slowly with Λ down to a few MeV.

Corrections. Let us now turn to the corrections that will enable us to extend the calculation to *all* points with $x \leq 0.032$, $Q^2 \geq 12\,\mathrm{GeV}^2$ (Fig. 1). We take them into account semi-phenomenologically[5] by replacing (2.10a) with

$$F_S(x,Q^2) \simeq B_S \left\{1 + \frac{c_S \alpha_s}{4\pi}\right\} \mathrm{e}^{q_S \alpha_s/4\pi}\, \alpha_s^{-d_+}\, x^{-\lambda} (1-x)^{\nu(Q^2)}, \tag{3.2a}$$

and fixing $\nu(Q^2)$ so that, for small Q^2, we agree with the result of the counting rules for $x \to 1$ and, for large Q^2, we satisfy the momentum sum rule,

$$\int_0^1 \mathrm{d}x\, F_S(x,Q^2) \underset{Q^2\to\infty}{\to} \frac{3n_f}{3n_f + 16}.$$

[4] This is in fact the reason why we have given a variety of evaluations, and not just the best ones: to get a flavour for the systematic theoretical uncertainties.

[5] The similitudes and differences with the more phenomenological procedure of ref. 2 should be apparent.

Specifically, we choose

$$\nu(Q^2) = \nu_0 + \left\{ \frac{B_S[1 + c_S\alpha_s/4\pi]e^{q_S\alpha_s/4\pi}\Gamma(1+\lambda)[16+3n_f]}{3n_f\alpha_s^{d_+}} \right\}^{1/(1-\lambda)}, \qquad (3.2b)$$
$$\nu_0 = 7.$$

Note that this does *not* introduce any new parameter.

For F_{NS} we replace (2.6) by

$$F_{NS} \simeq B_{NS}\left\{1 + \frac{v_{NS}\alpha_s}{4\pi}\right\}\alpha_s^{-d_{NS}}x^\rho(1-x)^{\nu_{NS}}, \qquad (3.2c)$$

but, because the NS component is only relevant at small values of Q^2 we fix $\nu_{NS} = 3$ independent of Q^2 (actually, the χ^2 varies by less than one unit for $0 \le \nu_{NS} \le 4$). Then, we still write $F_2 = \langle e_q^2\rangle[F_S + F_{NS}]$, and, for neutrino scattering,

$$xF_3 = F_{NS}^{\rm odd}(x,Q^2) = B_{NS}\left\{1 + \frac{v_{NS}^{\rm odd}\alpha_s}{4\pi}\right\}\alpha_s^{-d_{NS}}x^\rho(1-x)^{\nu_{NS}}. \qquad (3.2d)$$

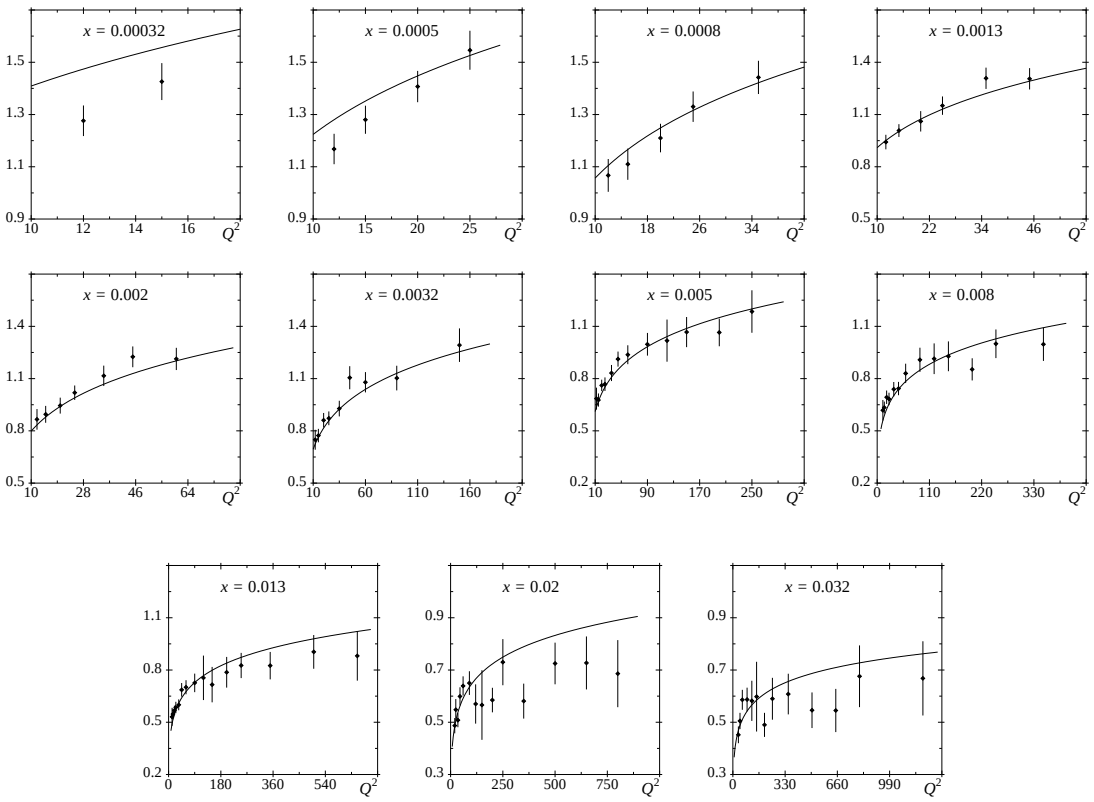

Figure 2a. Comparison of predictions from Eqs. (3.2a, c), Table V ($\Lambda = 0.14$ GeV), with H1 ep data[4] for F_2.

The results of the fit are presented in Table V, for the exponentiated expression, Eq. (3.2a). There is unfortunately no minimum as a function of Λ: the χ^2 decreases slowly with Λ. We thus give results only for two representative values of this parameter. The pictorial representation of the fit is given in Fig. 2a (for ep) and Fig. 2b for neutrino scattering, both for $\Lambda = 0.14\,\mathrm{GeV}$.

Table V. H1 plus ν data. $n_f = 4; x \leq 0.032,\ 12\ \mathrm{GeV}^2 \leq Q^2 \leq 1\,200\ \mathrm{GeV}^2$.

	λ	$\langle e_q^2\rangle B_S$	$\langle e_q^2\rangle B_{NS}$	χ^2/d.o.f.
$\Lambda = 0.10$ GeV :	0.3183	1.292×10^{-4}	0.328	$\frac{127.2}{110-3}$
$\Lambda = 0.20$ GeV :	0.3286	2.257×10^{-4}	0.371	$\frac{141.3}{110-3}$

The χ^2/d.o.f. is slightly larger than one. Part of the discrepancy is due to the data, some of which is clearly incompatible with the rest. Also, one may substantially improve the χ^2 if introducing a free parameter in the definition of $\nu(Q^2)$, as shown e.g. in ref. 2. However, part of the disagreement is certainly due to rigidity of the theoretical formulas, and to true deviation from the model which occur for "large" values of x. We will discuss this further in connection with the analysis of the Zeus data, and in Sect. 5.

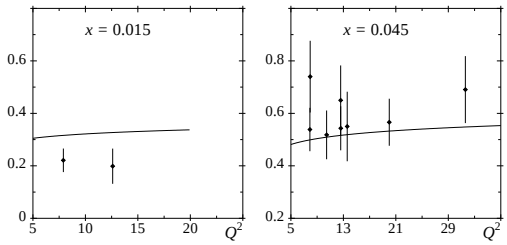

Figure 2b. Comparison of predictions from Eq. (3.2c), Table V ($\Lambda = 0.14$ GeV), with neutrino xF_3 data[15].

Finally, the fact that the χ^2 decreases with Λ past reasonable values is an indication that we are getting here an *effective* value for this parameter, which compensates for the large size of the NLO corrections.

We may consider fitting with the expanded version of the formula for F_S, i.e., with

$$F_S(x,Q^2) \simeq B_S \left\{1 + \frac{(c_S + q_S)\alpha_s}{4\pi}\right\} \alpha_s^{-d_+}\, x^{-\lambda}(1-x)^{\nu_{\mathrm{n.e.}}(Q^2)},$$

and now

$$\nu_{\mathrm{n.e.}}(Q^2) = \nu_0 + \left\{\frac{B_S\,[1 + (c_S + q_S)\alpha_s/4\pi]\,\Gamma(1+\lambda)[16 + 3n_f]}{3n_f\alpha_s^{d_+}}\right\}^{1/(1-\lambda)};$$

$$\nu_0 = 7.$$

The fit *deteriorates* clearly; the χ^2 is now of some 140, for 110-3 d.o.f. and $\Lambda = 0.10$. This shows that the exponentiated version of the formulas is to be preferred, as it probably sums at least part of the large NLO corrections. Because of this, we will henceforth use only the exponentiated version of the equations.

We next consider fits to the more recent Zeus data[4]. We will make two choices: first, we fit the neutrino data, and all ep points with $x \leq 0.01$ using the formula (2.10a). The results are given in Table VI. The chi-squared is reasonable, as is the value of Λ. The values of all parameters are compatible with those found from the fits to the H1 data. The second possibility is to extend the range to $x \leq 0.025$ and use Eq. (3.2), fixing $\Lambda = 0.135$. The results of the fit are shown in Fig. 3. We do not show the fit to the neutrino data, which does not differ substantially from that of Fig. 2b. The χ^2/d.o.f. is now of 226.1/(120-3). This, as the χ^2/d.o.f. reported for the fit of data with $x \leq 0.01$ in Table VI, are larger than their counterparts for the H1 data. A glance to Fig. 3 shows that part of the reason is the presence in the Zeus data of fluctuations. These are probably due to systematic errors not taken into account in the experimental analysis; they become important for very large Q^2. Thus, and although the Zeus data appear more precise than the H1 ones for the lower Q^2 range,[6] the last one are more reliable at large Q^2. Nevertheless, and as noted in the comments to the fit to H1 data, it is also clear that the theoretical predictions present *systematic* deviations from experiment, very likely due to the extension of the first beyond their range of validity by use of a semiphenomenological expression which is not sufficiently flexible; see Sect. 5 for more discussion. Apart from this, the results are good and the parameters of the fits reasonably compatible. The value of Λ is closer to the accepted one.

[6] This is probably the reason why the value of Λ deduced from the H1 data is *less* realistic than that obtained fitting the set of Zeus.

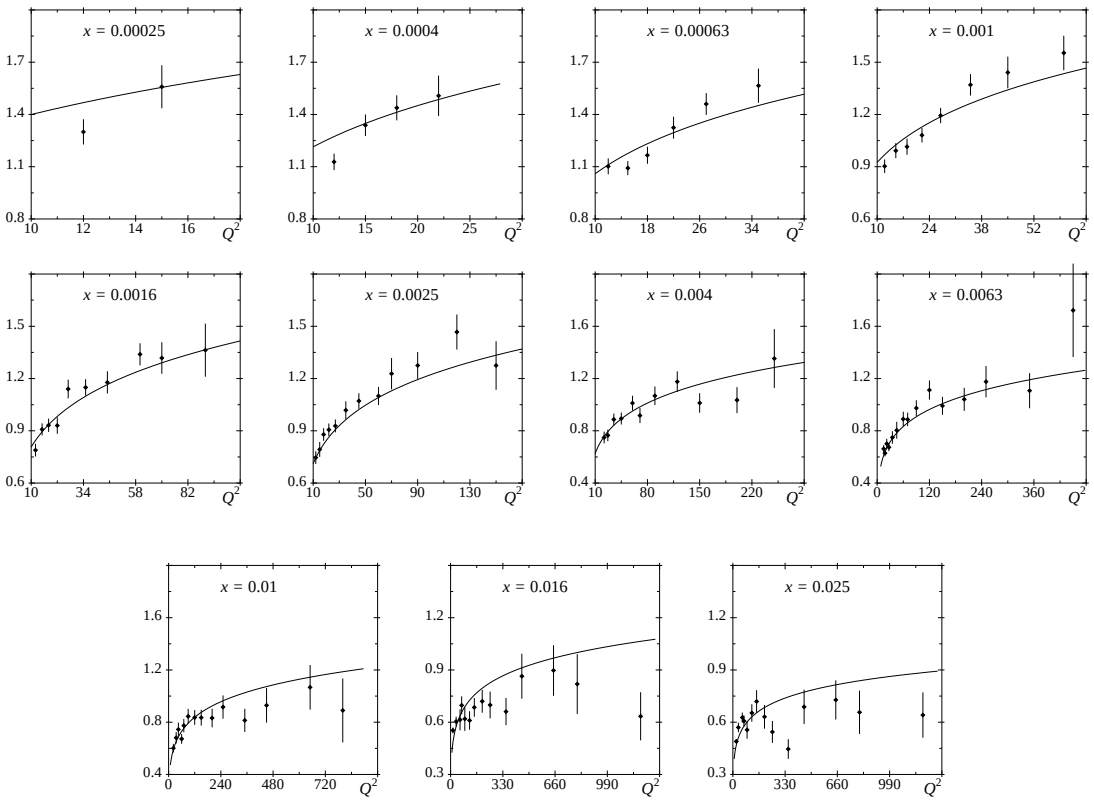

Figure 3. Comparison of predictions for F_2 from Eqs. (3.2a, c), $\Lambda = 0.135$, with Zeus ep data

Table VI. Zeus plus ν data. $n_f = 4$; $x \leq 0.01$.

Λ	λ	$\langle e_q^2 \rangle B_S$	$\langle e_q^2 \rangle B_{NS}$	χ^2/d.o.f.
$0.135^{+0.075}_{-0.055}$ GeV	0.301 ± 0.025	$1.250^{+0.552}_{-0.400} \times 10^{-4}$	0.3138 ± 0.007	$\frac{126.4}{92-4}$

As a final check on the reliability and consistency of the fits we have fitted Zeus data with $x \leq 0.01$, *not* including the neutrino data. We get no definite minimum for Λ, only constrained by $\Lambda \lesssim 0.2\,\mathrm{GeV}$; but we obtain values of the remaining parameters compatible with those obtained *including* xF_3, in particular a very reasonable value for B_{NS}:

$$\langle e_q^2 \rangle B_S = 1.8 \times 10^{-4}, \langle e_q^2 \rangle B_{NS} = 0.35, \lambda = 0.329.$$

In this sense we may say that our analysis is sufficiently precise to *predict* the NS structure functions from F_2 only, and this in spite of the relative smallness of F_{NS}. It is however clear that, as already mentioned several times, systematic deviations occur, especially large for $x \gtrsim 0.01$ (cf. Sect. 5).

3.2. The gluon structure function.

We give here the parametrizations to NLO for the gluon structure function that follow from our determination of the parameters in the previous subsection, for the full set of points corresponding to a set of parameters intermediate

between those given in Table V for F_2,

$$F_G(x,Q^2) = B_G\left[1+\frac{-0.25\alpha_s}{4\pi}\right]\mathrm{e}^{16.6\alpha_s/4\pi}\alpha_s(Q^2)^{-3.182}x^{-0.316}(1-x)^{\nu_G(Q^2)},$$

$$\nu_G(Q^2) = 5+\left\{\frac{B_G\,[1-0.25\alpha_s/4\pi]\mathrm{e}^{16.6\alpha_s/4\pi}\Gamma(1+0.316)[16+3n_f]}{16\alpha_s^{3.182}}\right\}^{\frac{1}{1-0.316}}, \qquad (3.5)$$

$$B_G = 25.2\times\langle e_q^2\rangle B_S,\ \langle e_q^2\rangle B_S = 1.226\times10^{-4},$$

$$\mathrm{NLO},\ x\le 3.2\times10^{-2},\ 12\,\mathrm{GeV}^2\le Q^2\le 1\,200\,\mathrm{GeV}^2;$$

$$n_f=4;\ \Lambda(2\,\mathrm{loop}, n_f=4) = 0.14\,\mathrm{GeV}.$$

The corresponding graphs are shown in Fig. 4, where we give both LO and NLO predictions, the LO calculation with values of parameters from Table I.

There are unfortunately no direct measurements of F_G with which to compare our calculations. *Indirect* estimates were made by the H1 collaboration, by fitting F_2, F_G with an exact coupled QCD evolution. The comparison with our calculations to LO may be found in ref. 1; the agreement is reasonable, and indeed our estimates are more precise than the DGLAP calculation, afflicted by large extrapolation errors.

More information on F_G is obtained from the cross-section $\gamma p\to J/\psi p$, to be discussed in Sect. 5.3.

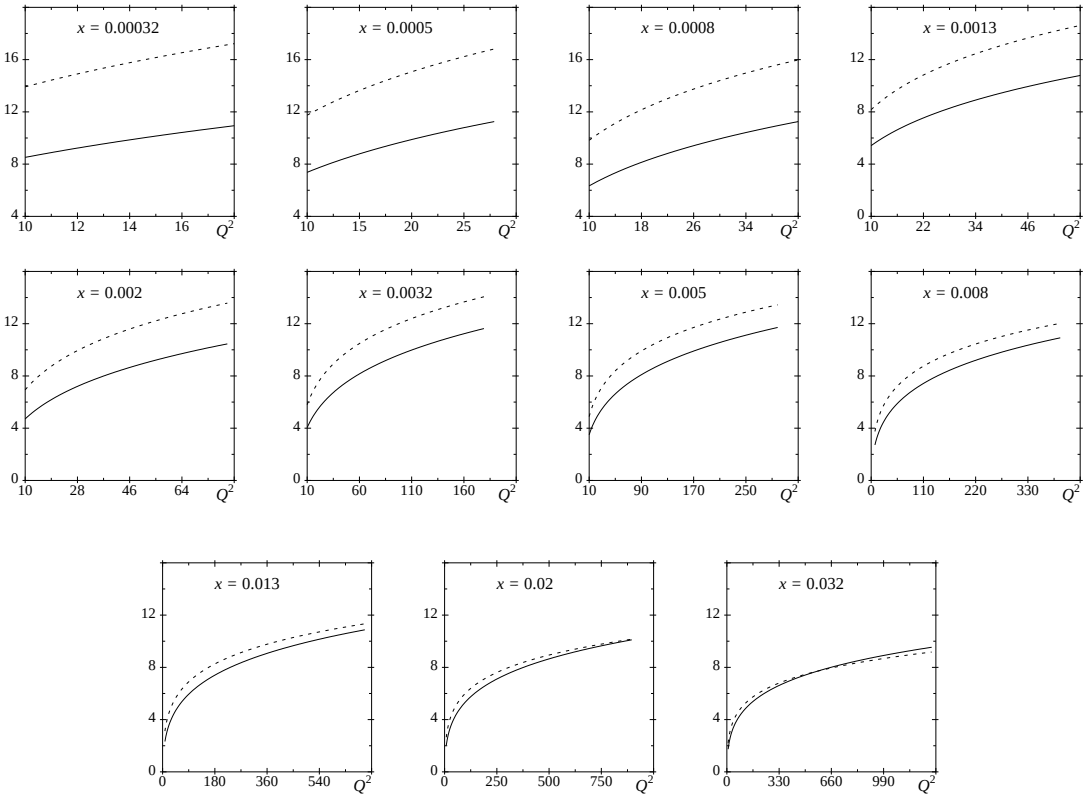

Figure 4. The gluon structure function F_G to LO (broken line), Eq. (3.3), and the optimum NLO one (continuous line), Eq. (3.5).

3.3. Predictions for the longitudinal structure function.

NLO, $O(\alpha_s^2)$ corrections to the longitudinal structure function are unfortunately *very* large; not because of the direct corrections, but due to corrections generated indirectly via the large NLO corrections to F_2. Indeed, the value of R' is reduced by more than a half from LO to NLO. We give in Fig. 5 a plot of LO and NLO calculations. Using Eq. (2.14), and the parameters $\Lambda = 0.20$, $\lambda = 0.38$ (Table I*a*) we get the LO result, $R^{(0)}$; and with Eqs. (2.15), (2.16) and the figures $\Lambda = 0.10,\ 0.20$ and $\lambda = 0.324$ (cf. Table IV*a*) we find R' (NLO). Also depicted are a few representative data. Note that the dependence of the NLO value of R on Λ is very slight, due to cancellation of various effects. Thus, the lines corresponding to $\Lambda = 0.10,\ 0.20$ in Fig. 5 fall almost one on top of the other.

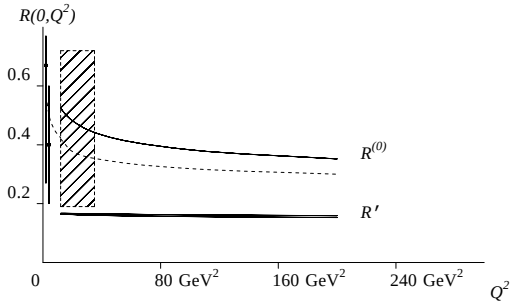

Figure 5. Predictions for $R'(0, Q^2)$ to LO and NLO. Hatched box: preliminary result from H1[17]. Dots: data from ref. 18 (actually, at $x \sim 0.05$). Discontinuous line: intermediate calculation, see main text.

To get a further indication on the meaning of the results, we have also calculated R' from the effective fit at low energy of ref. 1, with $\lambda = 0.324$, and α_s to two loops, but without other NLO corrections, taking $n_f = 3$ below $Q^2 = 12\ \mathrm{GeV}^2$, and $n_f = 4$ above. This is the intermediate, dashed curve in Fig. 5. Clearly, one would expect that the real R' would somehow interpolate between this, at low momentum, and the full NLO curve, for very large Q^2. The predictions should be checked against experiment when, and if, measurements independent of those of F_2 are performed at HERA. We have given the predictions for $x = 0$; the figures would not change much provided $x \leq 10^{-2}$.

4. THE SOFT-POMERON DOMINATED MODEL

As remarked in the Introduction, the results derived in the previous sections assume that the singlet structure functions are dominated, at small x, by the singularities of the matrix elements of the quark and gluon operators. We may instead hypothesize that these singularities lie to the left of $n = 1$, and then the small x behaviour is controlled by the singularities of the Wilson coefficients. Specifically, this occurs if one assumes that, for all Q^2 below a certain Q_0^2 of the order of a typical hadronic scale (say $\sim$ GeV), cross sections behave according to a standard soft-Pomeron dominance,

$$\sigma_{\mathrm{tot}}(Q_0^2, s) \simeq \mathrm{Constant},$$

for $Q_0^2 \lesssim 1\ \mathrm{GeV}^2$.

We can then get the structure functions for small x by evolving with QCD the expressions corresponding to this,[9,10,11]

$$F_i(x, Q_0^2) \underset{x \to 0}{\simeq} c_i,\ i = S, G. \tag{4.1}$$

We will present a sketchy derivation of the resulting formulas, to NLO. This is of interest because we use the moments method, instead of the Altarelli-Parisi equations employed in ref. 11, so we have a nontrivial check of the calculation there.

4.1. Theoretical calculations: F_S and F_G

Our starting point is the following relation, proved in ref. 6 to NLO,

$$\alpha_s(Q^2)^{\hat{\mathbf{D}}}(1 + a\boldsymbol{\Gamma})\mathbf{S}^{-1}(1 - a\mathbf{C}^{(1)})\boldsymbol{\mu}(n, Q^2) \equiv \mathbf{b} = \text{independent of } Q^2. \tag{4.2}$$

Here $a = \alpha_s(Q^2)/4\pi$, $\mathbf{C}^{(1)}$ is the matrix of NLO corrections to the Wilson coefficients[7] and

$$\alpha_s^{\hat{\mathbf{D}}} = \begin{pmatrix} \alpha_s^{d_+} & 0 \\ 0 & \alpha_s^{d_-} \end{pmatrix}, \ \mathbf{\Gamma} = -\frac{1}{2\beta_0} \begin{pmatrix} \bar{\gamma}_{11}(n) + 2\beta_1 d_+(n) & \dfrac{\bar{\gamma}_{12}(n)}{d_+(n) - d_-(n) + 1} \\ \dfrac{\bar{\gamma}_{21}(n)}{d_-(n) - d_+(n) + 1} & \bar{\gamma}_{22}(n) + 2\beta_1 d_-(n) \end{pmatrix} \tag{4.3}$$

with $\mathbf{S}$, $\bar{\gamma}$ defined before; explicit expressions for these quantities may be found in the Appendix. Here we only give the values, in the limit $n \to 1$, of those of interest for us now. We have:

$$\begin{aligned} d_+(n) \simeq \frac{d_0}{4(n-1)} - d_1, \ d_-(n) \simeq -\frac{16 n_f}{27\beta_0}, \\ d_0 = \frac{48}{\beta_0}, \ d_1 = \frac{11 + \frac{2}{27} n_f}{\beta_0}; \\ \mathbf{S}(n) \simeq \begin{pmatrix} 1 & -\dfrac{n_f(n-1)}{9} \\ \dfrac{9}{n_f(n-1)} & \dfrac{4 n_f (n-1)}{81} \end{pmatrix}, \end{aligned} \tag{4.4a}$$

and, defining $\gamma_{ij}(n) \simeq r_{ij}/(n-1)$,

$$\begin{aligned} r_{12} = -\tfrac{320}{9} n_f T_F C_A, \\ r_{22} = \tfrac{368}{9} n_f T_F C_A - \tfrac{32}{3} n_f T_F C_F. \end{aligned} \tag{4.4b}$$

Finally,

$$\begin{aligned} C_{11}^{(1)}(n) \simeq C_F[\pi^2 - \tfrac{17}{2} - 4\zeta(3)](n-1), \ C_{12}^{(1)}(n) \simeq \tfrac{4}{3} n_f T_F \\ C_{21}^{(1)}(n) \simeq \frac{16 T_F}{3(n-1)}, \ C_{22}^{(1)}(n) \simeq \frac{12 T_F}{n-1}. \end{aligned} \tag{4.4c}$$

In the soft Pomeron hypothesis the behaviour of $F_{S,G}$ as $x \to 0$ is, as discussed, dominated by the singularities of the $\mathbf{C}^{(1)}(n)$, $\boldsymbol{\gamma}^{(0)}(n)$, $\boldsymbol{\gamma}^{(1)}(n)$ as $n \to 1$, which in turn give those of the $\boldsymbol{\mu}(n)$. From (4.2 - 4) one easily finds,

$$\begin{aligned} \boldsymbol{\mu}(n, Q^2) \underset{n\to 1}{\simeq} b_1 \alpha_s^{-d_+(n)} \begin{pmatrix} 1 + \dfrac{a k_1}{n-1} \\ \dfrac{9}{n_f(n-1)} \left\{ 1 + \dfrac{ak}{n-1} \right\} \end{pmatrix}, \\ k = 12 T_F + \frac{1}{2\beta_0} \left(\tfrac{4}{9} r_{12} + r_{22} + \frac{24\beta_1}{\beta_0} \right), \ k_1 = k - \frac{3 r_{12}}{8 n_f}. \end{aligned} \tag{4.4d}$$

Note that, because for $n \to 1$, $d_+(n) \gg d_-(n)$, only the term in $\alpha_s^{-d_+(n)}$ (and not that in $\alpha_s^{-d_-(n)}$) contributes.

Next we evaluate b_1 in terms of $F_i(x, Q_0^2)$, assumed to behave as in (4.1) so that

$$\mu_i(n, Q_0^2) \underset{n\to 1}{\simeq} c_i \frac{1}{n-1}. \tag{4.5}$$

This is accomplished using again (4.2) for $Q = Q_0$, profiting from the independence of b_1 on Q^2. The computation is straightforward and we find

$$\begin{aligned} b_1 = \alpha_s(Q_0^2)^{d_+(n)} \left\{ 1 - \frac{\alpha_s(Q_0^2) k}{4\pi(n-1)} \right\} c_0, \\ c_0 = n_f \left[\tfrac{4}{81} c_1 + \tfrac{1}{9} c_2 \right]. \end{aligned} \tag{4.6}$$

[7] Defined as in ref. 6, which fixes the arbitrariness in F_G.

Plugging the result into (4.4) we get

$$\begin{aligned}\boldsymbol{\mu}(n,Q^2) &\underset{n\to 1}{\simeq} c_0 \mathrm{e}^{\tau d_0/4(n-1)-\tau d_1}\\ \times\begin{pmatrix} 1+\left[k-\dfrac{3r_{12}}{8n_f}\right]\dfrac{\alpha_s(Q^2)}{4\pi(n-1)}-k\dfrac{\alpha_s(Q_0^2)}{4\pi(n-1)} \\ \dfrac{9}{n_f(n-1)}\left\{1+k\dfrac{\alpha_s(Q^2)}{4\pi(n-1)}-k\dfrac{\alpha_s(Q_0^2)}{4\pi(n-1)}\right\}\end{pmatrix}&,\qquad (4.7)\\ \tau=\log\frac{\alpha_s(Q_0^2)}{\alpha_s(Q^2)}&,\end{aligned}$$

with d_0, d_1 as in (4.4a). We then invert the Mellin transform. Generally, if

$$\mu(n)=\int_0^1 \mathrm{d}x\; x^{n-1}F(x), \qquad (4.8a)$$

and

$$\mu(n)\simeq\frac{1}{(n-1)^\nu}\mathrm{e}^{d_0\tau/4(n-1)} \qquad (4.8b)$$

then

$$F(x)\underset{\substack{x\to 0\\ \tau\to\infty}}{\simeq}\xi^\sigma f_\sigma(\tau)\mathrm{e}^{\sqrt{d_0\tau\xi}} \qquad (4.9)$$

where[8]

$$\xi=\log x^{-1},\ \sigma=\tfrac{1}{2}\nu-\tfrac{3}{4},\ f_\sigma(\tau)=\frac{4^\sigma}{\pi^{\frac{1}{2}}}(d_0\tau)^{-\sigma-\frac{1}{2}}. \qquad (4.10)$$

The proof is elementary and is obtained by substituting (4.9) in (4.8a) and integrating. Thus we get the final result,

$$\begin{aligned}F_S(x,Q^2)&\underset{\substack{x\to 0\\ Q^2\gg Q_0^2}}{\simeq} c_0\xi^{-1}\left(\frac{d_0\tau\xi}{64\pi^2}\right)^{\frac{1}{4}}\exp\left[\sqrt{d_0\tau\xi}-d_1\tau\right]\\ &\times\left\{1+2\sqrt{\frac{\xi}{d_0\tau}}\left[k_1\;\frac{\alpha_s(Q^2)}{4\pi}-k(1+\delta)\;\frac{\alpha_s(Q_0^2)}{4\pi}\right]\right\},\qquad (4.11a)\\ F_G(x,Q^2)&\underset{\substack{x\to 0\\ Q^2\gg Q_0^2}}{\simeq}\frac{9c_0}{n_f}\frac{1}{(4\pi^2 d_0\tau\xi)^{\frac{1}{4}}}\exp\left[\sqrt{d_0\tau\xi}-d_1\tau\right]\\ &\times\left\{1+2\sqrt{\frac{\xi}{d_0\tau}}\left[k\;\frac{\alpha_s(Q^2)}{4\pi}-k(1+\delta)\;\frac{\alpha_s(Q_0^2)}{4\pi}\right]\right\}.\qquad (4.11b)\end{aligned}$$

Here k, k_1 are given in (4.4d) with the r_{ij} of (4.4b). We have added an arbitrary factor $(1+\delta)$ for reasons that will be clear later. In the soft Pomeron model, one of course has $\delta=0$. Numerically,

$$\begin{aligned}k_1&=k-3r_{12}/8n_f\simeq 42.19\\ k&\simeq 22.19\ (\text{both for } n_f=4).\end{aligned} \qquad (4.11c)$$

Eq. (4.11a) may be compared with the calculation of Ball and Forte.[11] We agree in the LO term, and in the coefficient of $\alpha_s(Q^2)/4\pi$ in the NLO term, but disagree in the coefficient of the $\alpha_s(Q_0^2)/4\pi$ term. This is not of great moment[9] since the numerical difference is slight, 22.19 *vs* 16.19. Eq. (4.11b) is given here for the first time.

NLO corrections are *very* large. Indeed, for fixed Q^2, $x\to 0$, the NLO correction overwhelms the LO part. This, together with the problem posed by the BFKL-Florentine terms[19,20]

$$x^{-\omega_0\alpha_s(\nu^2)};\ \omega_0=\text{Constant}$$

[8] From (4.8 to 10) it thus follows that powers of $n-1$ correspond to powers of $\sqrt{|\log x|}$. Therefore, we cannot, unless a more definite assumption is made about the behaviour of the structure functions at Q_0^2, give results more precise than terms of relative order $1/\sqrt{|\log x|}$.

[9] Nevertheless an independent calculation that resolved the discrepancy would be welcome.

will be discussed in Sect. 5.

4.2. Theoretical calculations: longitudinal structure function.

We define as before (Sect. 2.3) $R' \simeq F_L/F_S$. Because, in the soft Pomeron dominated model, the contribution to F_L of F_S is subleading with respect to that of F_G in the $x \to 0$ limit, it follows that we may, to errors of relative size $\sqrt{1/|\log x|}$, neglect the contribution of F_S to F_L. For completeness, however, we will give the formula including this contribution of F_S. We then have an equation similar to (2.13),

$$F_L(x,Q^2) \simeq F_G(x,Q^2)\int_0^1 \mathrm{d}y\; C_G^L(y,Q^2) + F_S(x,Q^2)\int_0^1 \mathrm{d}y\; C_S^L(y,Q^2), \tag{4.12}$$

and the C^L are as in (2.12b).

We let

$$\begin{aligned} I_g(x) &= T_F n_f [C_F I_{G1}(0) + C_A I_{G2}(0;x)] \simeq -17.62 - \frac{32 n_f T_F C_A}{9}\log x^{-1}, \\ I_q(x) &= C_F(C_A - 2C_F) I_{S1}(0) + C_F^2 I_{S2}(0) + C_F T_F n_f I_{S3}(0) + C_F T_F n_f I_{PS}(0;x), \end{aligned} \tag{4.13}$$

where

$$\int_x^1 \mathrm{d}y c_G^{(1)L}(y) \equiv n_f T_F [C_F I_{G1}(0) + C_A I_{G2}(0;x)],$$

and similar expressions for the I_S, I_{PS}. We then obtain the NLO expression for R',

$$\begin{aligned} R'(x,Q^2) \underset{\substack{x\to 0\\ Q^2\gg Q_0^2}}{\simeq} &\left\{ 2C_F + I_q \frac{\alpha_s(Q^2)}{4\pi} \right. \\ &\left. + 48 T_F \sqrt{\frac{\xi}{d_0\tau}} \Big[1 + \big(-\tfrac{80}{3} T_F C_A \sqrt{\frac{\xi}{d_0\tau}} + \tfrac{3}{8} I_g \big) \frac{\alpha_s(Q^2)}{4\pi} \Big] \right\} \frac{\alpha_s(Q^2)}{4\pi}. \end{aligned} \tag{4.14}$$

Because the NLO corrections are so large, we will use, instead of (4.14), a nonexpanded version for comparison with experiment. Removing also the NLO contribution of F_S the formula to be employed for numerical calculations is then,

$$\begin{aligned} R'(x,Q^2) \underset{\substack{x\to 0\\ Q^2\gg Q_0^2}}{\simeq} &\left[48 T_F \sqrt{\frac{\xi}{d_0\tau}} + 2C_F \right] \frac{1 + \left(2k\sqrt{\xi/d_0\tau} \right) \alpha_s(Q^2)/4\pi}{1 + \left(2k_1\sqrt{\xi/d_0\tau} \right) \alpha_s(Q^2)/4\pi} \\ &\times \left\{ 1 + \tfrac{3}{8} I_g(x)\, \frac{\alpha_s(Q^2)}{4\pi} \right\} \frac{\alpha_s(Q^2)}{4\pi}. \end{aligned} \tag{4.15}$$

4.3. Comparison with experiment.

For the soft Pomeron dominated model a very peculiar phenomenon occurs: the LO expressions produce fits *better* than the NLO ones. What is more, and unlike in the hard singularity case where we could blame the discrepancy on the large x points, here it is uniformly distributed. The strategy for comparison with experiment should be different now. First of all, we will not include a term like $(1-x)^\nu$ connected with the saturation of the momentum sum rule since it is now very small, and would arrange nothing. Secondly, we give parameters for the LO fit for the restricted ($x \le 0.01$) range, and we give results of the NLO calculation both for the restricted ($x \le 0.01$) and full ranges. These we will discuss in greater detail.

As stated we begin a LO calculation, fixing $\Lambda(1\text{ loop } n_f = 4) = 0.20\ \mathrm{GeV}$, and taking for definiteness the H1 data, plus the neutrino data for stability. We find the results of Table VII*a*.

Table VII*a*. LO calculation; $x \leq 0.01$, H1 plus ν data.

$\langle e_q^2 \rangle c_0$	$\langle e_q^2 \rangle B_{NS}$	Q_0^2	χ^2/d.o.f.
0.12	0.44	0.46 GeV^2	$\frac{48.2}{68-3}$

We consider next the NLO calculation which we split into two parts: restricted range, and full range. For the first we give the results of the calculation in Table VII*b*. Only the H1 data are considered, for comparison with Table VII*a*. We *do* include neutrino data to force reasonable values for B_{NS}.

Table VII*b*. NLO calculation; $x \leq 0.01$, H1 plus ν data.

Λ	$\langle e_q^2 \rangle c_0$	$\langle e_q^2 \rangle B_{NS}$	Q_0^2	χ^2/d.o.f.
0.160^{+70}_{-60}GeV	0.292 ± 0.001	0.326 ± 0.020	$0.86^{+0.40}_{-34}$ GeV^2	$\frac{74.3}{68-4}$

As mentioned, the chi-squared has clearly deteriorated,[10] although the values of Q_0^2, B_{NS} are more realistic now. The value of Λ, also fitted, is reasonable.

For the full range we give the results of the fits to both H1 and Zeus data in Tables VIII. For the H1 set there is no reasonable minimum for Λ; for Zeus the optimum is for $\Lambda = 0.165\,\mathrm{GeV}$. Thus we fix this value for both sets of data.

Table VIII*a*. NLO calculation; Zeus plus ν data, $x \leq 0.025$, $\Lambda = 0.165\,\mathrm{GeV}$

$\langle e_q^2 \rangle c_0$	$\langle e_q^2 \rangle B_{NS}$	Q_0^2	χ^2/d.o.f.
0.282	0.240	0.90 GeV^2	$\frac{273.2}{120-4}$

Table VIII*b*. NLO calculation; H1 plus ν data, $x \leq 0.032$, $\Lambda = 0.165\,\mathrm{GeV}$

$\langle e_q^2 \rangle c_0$	$\langle e_q^2 \rangle B_{NS}$	Q_0^2	χ^2/d.o.f.
0.265	0.246	0.70 GeV^2	$\frac{190.6}{110-4}$

Our results are consistent among themselves, and with an existing NLO calculation, based on H1 data[21]; the comparison with the Zeus data for $x \leq 0.025$ is shown in Fig. 6.

[10] For Zeus data we would have had a much worse figure, χ^2/d.o.f.=$\frac{180.5}{92-4}$, but a slightly better $\Lambda = 0.20$. The other parameters do not change substantially.

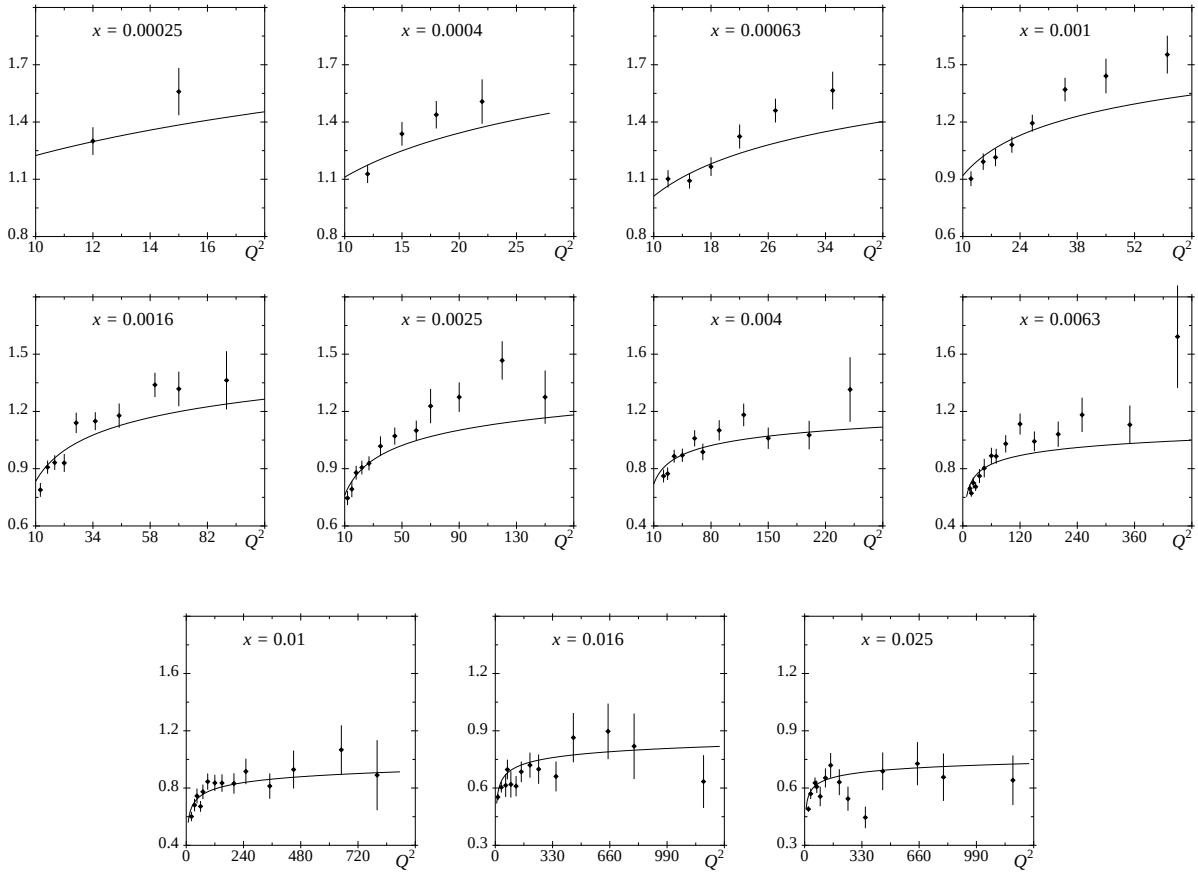

Figure 6. Predictions for the structure function F_2 to NLO in the soft-Pomeron model, and Zeus data.

The results may be confronted with the ones obtained if *not* including the NLO correction: we would have obtained, for the generally preferred value $\Lambda = 0.23\,\mathrm{GeV}$,

$$\chi^2/\mathrm{d.o.f.} = \frac{142.1}{120-3}\ (\mathrm{Zeus})$$
$$\chi^2/\mathrm{d.o.f.} = \frac{90.0}{110-3}\ (\mathrm{H1}).$$

The situation is somewhat unpleasant. To make it worse, we mention that, if we delete the term in $\alpha_s(Q_0^2)$ in Eq. (4.11a), by simply putting $\delta = -1$ there, the quality of the fit *improves* substantially: to a chi-squared/d.o.f. of $\frac{141.4}{120}$ for Zeus data, and $\frac{78.1}{110-3}$ for H1, with $\Lambda = 0.23\,\mathrm{GeV}$.

It is difficult to draw a clear-cut conclusion from this. At any rate, in all cases the fits are comparable in quality to those obtained with the hard singularity hypothesis, and reasonably good; more discussion will be given in Sect. 5.

For the longitudinal function, the predictions and comparison with experiment are depicted in Fig. 7; both the LO prediction based on the parameters of Table VII, and the NLO ones using the figures from Table VIIIa. Like in the hard singularity case, and for the same reason (large size of NLO corrections to F_S) there is a dramatic decrease between LO and NLO predictions, particularly for "large" values of x, and for *very* small ones. NLO results, depicted for various values of x in the figure are below the data. One cannot, nevertheless, consider the disagreement with experiment to be serious given the errors both of it and of the theory. Perhaps more serious is the problem that the NLO corrections also here overwhelm the LO piece for $x \to 0$.

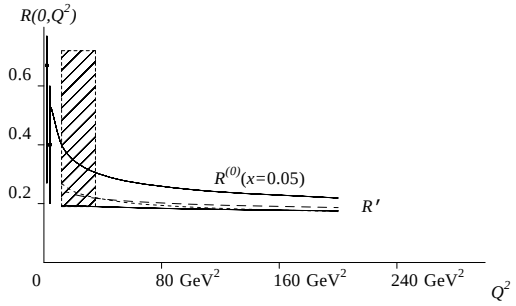

Figure 7. Predictions for $R'(x,Q^2)$ to LO and NLO, soft Pomeron model. R': dotted, $x = 0.05$; dashed line: $x = 10^{-3}$; continuous line: $x = 10^{-4}$. Hatched box: ref. 17 ($x \sim 10^{-3}$). Dots: data from ref. 18 at $x \sim 0.05$.

5. HARD PLUS SOFT SINGULARITIES. LARGE Q^2.

5.1. Discussion.

It may appear strange that two mutually contradictory hypotheses, leading to so apparently different behaviours as the soft and hard Pomeron ones, produce both results in fair agreement with the data. The reason, however, is not difficult to find: both behaviours solve the QCD evolution equations, so the agreement of the calculations with experiment only depends essentially on the theoretical formulas fitting experiment at *one* value Q_1^2, say $Q_1^2 = 12\ \mathrm{GeV}^2$, and on the validity of QCD for the subsequent evolution for larger Q^2 at small x. However, neither the hard nor the soft Pomeron solution are fully satisfactory. The hard Pomeron expression fails to fit data with $x \gtrsim 0.01$. The soft Pomeron does not produce a marvellous fit either, and in addition presents conceptual problems, that we now briefly discuss.

First of all, we have the problem that, in the soft Pomeron case, the NLO overwhelms the LO term for small x (as $\sim \alpha_s\sqrt{\log x}$), so the soft Pomeron-inspired formulas must necessarily fail for the strict $x \to 0$ limit. This is not the case for the hard singularity behaviour. Secondly, a power behaviour seems to be indicated for consistency with the $\gamma^*\gamma$ scattering case, where it has been shown to occur[22]. Finally, we have the following argument. By Reggeon calculus methods or summing ladder graphs, the authors of refs. 19, 20 have, at *tree* level, found the behaviour

$$F_S \sim x^{-\omega_0 \alpha_s(\mu^2)},\ \omega_0 = \frac{4C_A \log 2}{\pi}.$$

This poses no threat to the hard singularity behaviour since this term is subdominant with respect to $x^{-\lambda}$ if, as seems natural, the argument of α_s is proportional to Q^2; but it is incompatible with the soft Pomeron hypothesis because the new term dominates it. (However, there is a way out if the argument of α_s was the *hadronic* energy, $s \sim Q^2/x$ for then, as $x \to 0$, the new term would become merely a constant).

A possibility that allows us to keep the best of both worlds is that one has, at a low Q_0^2, a behaviour sum of the hard and soft Pomeron ones,

$$F_S(Q_0^2, x) \simeq c + bx^{-\lambda}.$$

Although this implies that in the limit $x \to 0$ the hard singularity will dominate, for finite x, if $c \ll b$, both soft and hard singularities may contribute comparable amounts. In this context it may be remarked that a behaviour like the one above has been shown[23,1] to describe very well photoproduction ($Q^2 = 0$) with constants precisely in the relation $c \ll b$. If this persists up to $Q_0^2 \sim$ a few GeV^2, the mixed behaviour would be indicated. Needless to say, since both soft and hard-singularity dominated behaviours fit the data a mixed one will do so even better: for example, the deficiencies of the hard singularity picture at "large" x, and of the soft Pomeron one at all x, discussed in connection

with the fit to the Zeus data, would likely be at least partially cured.[11] The conceptual difficulties of the soft Pomeron term alone also disappear as, in the strict limit $x \to 0$, it is dominated by the hard piece.

There exists also a theoretical argument in favour of the hard plus soft Pomeron situation, and it comes from multi-Pomeron exchange theory. If, at a fixed Q^2 of the order of the GeV a single hard Pomeron gives[12]

$$F_{1P}(x,Q^2) \underset{s\to\infty}{\simeq} b_{1P}(Q^2)s^{\lambda},$$
$$s \equiv Q^2/x,$$

then an n-Pomeron term will produce the behaviour

$$F_{nP}(x,Q^2) \underset{s\to\infty}{\simeq} b_{nP}(Q^2)s^{n\lambda};$$

the constants b_{nP} should depend on the momentum at which they are calculated.

In some approximations (e.g., of eikonal type[24]) one has, for $Q^2 = -M^2_{\rm had}$, i.e., for on-shell scattering of hadrons,

$$b_{nP}(-M^2_{\rm had}) = (-1)^{n+1}\frac{\kappa^n}{n!}C,$$

so we get for the sum

$$\begin{aligned} F_S(x,-M^2_{\rm had}) &= \sum_{n=1}^{\infty} F_{nP}(x,Q^2=-M^2_{\rm had}) \\ &= C - C\exp\left[-\kappa s^{\lambda}\right] \underset{s\to\infty}{\simeq} C. \end{aligned}$$

For values of Q^2 of the order of $Q_0^2 \sim 2 - 4\,\mathrm{GeV}^2$, we expect that the $b_{nP}(Q^2)$ will not change much from $b_{nP}(-M^2_{\rm had})$, so if we write

$$b_{nP}(Q_0^2) \simeq b_{nP}(-M^2_{\rm had}) + \Delta_n,$$

we will then get,

$$F_S(x,Q_0^2) \simeq F_S(x,-M^2_{\rm had}) + \sum \Delta_n \simeq C + \Delta_1 x^{-\lambda} + \Delta_2 x^{-2\lambda} + \ldots, \tag{5.1}$$

with the Δ small. This expression contains a hard plus a soft Pomeron of the type discussed above. It also contains a term $\Delta_2 x^{-2\lambda}$, whose inclusion we will consider in Sect. 5.3.

5.2. Hard plus soft singularities for F_2.

We next discuss the large $Q^2 \gtrsim 10\,\mathrm{GeV}^2$ region, under various hypotheses for the small Q^2 region, which we then evolve with QCD. We will consider moderately large values of x, $x \leq 0.032$ because we will be interested not only on the leading behaviour as $x \to 0$, given almost certainly by a hard singularity, but also on the subleading corrections. So we assume that at a certain, fixed $Q_0^2 \sim 1\,\mathrm{GeV}^2$, one has

$$F_S\,(x,Q_0^2) \simeq B_S\,x^{-\lambda} + F_{\rm corr.}(x,Q_0^2). \tag{5.2}$$

For the correction term, $F_{\rm corr.}(x,Q_0^2)$, we consider the following possibilities: a soft Pomeron,

$$F^P_{\rm corr.}(x,Q_0^2) \simeq \text{constant}; \tag{5.3a}$$

and a P' Regge pole,[13]

$$F^{P'}_{\rm corr.}(x,Q_0^2) \simeq \text{constant} \times x^{1-\alpha_{P'}(0)}, \alpha_{P'}(0) \sim 0.5. \tag{5.3b}$$

This last possibility is considered because, as shown in ref. 10, any behaviour x^{σ}, $\sigma \geq 0$ at Q_0^2, produces at larger Q^2 behaviours differing from the soft Pomeron one, (1.4a), *only in the pre-factor*, but with the same exponent.

Once assumed the behaviours given in (5.3), and taking for simplicity that the gluon structure function behaves like the quark singlet one, we evolve with QCD for higher Q^2. From the results of the previous Sects. we find, to NLO,

$$F_S(x,Q^2) \simeq B_S\left\{1 + \frac{c_S(1+\lambda_0)\alpha_s}{4\pi}\right\} \mathrm{e}^{q_S(1+\lambda_0)\alpha_s/4\pi}[\alpha_s(Q^2)]^{-d_+(1+\lambda_0)}x^{-\lambda_0} + F_{\rm corr.}(x,Q^2), \tag{5.4}$$

[11] The hard singularity picture overshoots the large x, Q^2 data (Fig. 3) while the soft Pomeron one undershoots the small x points, and undershoots large x ones: see Fig. 6.

[12] The following discussion is rather sketchy; details and references may be found in the review of ref. 24.

[13] For Regge pole theory cf. ref. 25.

and depending on the low Q_0^2 hypothesis we make we find the following correction terms:

$$F^P_{\rm corr.}(x,Q^2) \simeq \left\{1+2\sqrt{\frac{\xi}{d_0\tau}}\left[k_1\,\frac{\alpha_s(Q^2)}{4\pi}-k\,\frac{\alpha_s(Q_0^2)}{4\pi}\right]\right\} \times\frac{c_0}{\xi}\left[\frac{9\xi\tau}{4\pi^2(33-2n_f)}\right]^{\frac{1}{4}}\exp\left\{\sqrt{d_0\xi\,\tau}-d_1\tau\right\} \tag{5.5a}$$

for a soft Pomeron, Eq. (5.3a). For the P' Regge pole we find a very similar formula:

$$F^{P'}_{\rm corr.}(x,Q^2) \simeq \left\{1+2\sqrt{\frac{\xi}{d_0\tau}}\left[k_1\,\frac{\alpha_s(Q^2)}{4\pi}-k\,\frac{\alpha_s(Q_0^2)}{4\pi}\right]\right\} \times\frac{c_{P'}}{\sqrt{\xi}}\left(\frac{\tau}{\xi}\right)^{\frac{3}{4}}\exp\left\{\sqrt{d_0\xi\,\tau}-d_1\tau\right\}. \tag{5.5b}$$

As we will see, none of the three possibilities gives a really good fit in the "large" $0.01 < x \leq 0.032$ region; for the more precise Zeus data the χ^2/d.o.f. is of 1.7. To remedy this we consider the possibility of softening the large x region by multiplying $F_S(x,Q^2)$ by a factor $(1-x)^\nu$, as discussed in Sect. 3. Here, however, we take ν constant because this already produces an excellent fit.

The results are summarized in Table IX, where for definiteness we compare the fits obtained with (5.5a,b) with the fits found using only the soft Pomeron-dominated expression. We have *not* fitted λ, which we have set equal to 0.470, for reasons that will be apparent in next section; if we had fitted it, we would have obtained $\lambda = 0.43$ and an improvement of only two units in the chi-squared[14]. We give the results for the Zeus data only; later we will present simultaneous fits to H1 and Zeus data.

Table IX.- $n_f = 4$; Zeus data, plus neutrino data. $x \leq 0.025$, $Q^2 \geq 12.5\,\mathrm{GeV}^2$

Soft Pomeron only	Λ	Q_0^2	$\langle e_q^2\rangle c_0$	$\langle e_q^2\rangle B_{NS}$	χ^2/d.o.f.	
	0.165 GeV	0.90 GeV^2	0.282	0.240	$\frac{273}{120-4}$	
Hard + Soft Pomeron*	λ (fixed)	Q_0^2	$\langle e_q^2\rangle c_0$	$\langle e_q^2\rangle B_S$	$\langle e_q^2\rangle B_{NS}$	χ^2/d.o.f.
	0.47	2.45 GeV^2	0.252	4.42×10^{-4}	0.294	$\frac{197}{120-4}$
Hard + P'*, large x softened**	λ (fixed)	Q_0^2	$\langle e_q^2\rangle c_{P'}$	$\langle e_q^2\rangle B_S$	$\langle e_q^2\rangle B_{NS}$	χ^2/d.o.f.
	0.47	1.11 GeV^2	0.616	4.25×10^{-4}	0.343	$\frac{171}{120-4}$
Hard + Soft*, large x softened	λ (fixed)	Q_0^2	$\langle e_q^2\rangle c_0$	$\langle e_q^2\rangle B_S$	$\langle e_q^2\rangle B_{NS}$	χ^2/d.o.f.
	0.47	2.72 GeV^2	0.310	3.417×10^{-4}	0.370	$\frac{143}{120-4}$

* Λ fixed at 0.230 GeV. The optimum value would correspond to $\Lambda \sim 0.45$ GeV.
** If we had not corrected for the large x values, i.e., we had not included the factor $(1-x)^\nu$, we would have obtained a χ^2/d.o.f. of 270.

In this table the expression "large x softened" means that we have multiplied the formulas for F_S by a factor $(1-x)^\nu$, $\nu \simeq 11$, to correct the structure functions for (relatively) large values of x. For the hard singularity case, cf. ref. 5 and Sect. 3.4 here; for the Hard + Soft singularities case, we have taken $\nu = 10 \sim 11$. (We will discuss further the "large" x region in Sect. 5.3).

5.3. Hard plus soft singularities, plus triple Pomeron term for F_2. Best (global) fits.

[14] To be precise, if we had *fitted* λ to e.g., the Zeus data using a hard plus soft term, we would have obtained (not correcting for large x, and fixing $\Lambda = 0.23\,\mathrm{GeV}$),

$$\lambda = 0.429,\ Q_0^2 = 2.40\ \mathrm{GeV}^2,\ \langle e_q^2\rangle c_0 = 0.244,\ \langle e_q^2\rangle B_S = 3.83\times10^{-4},\ \langle e_q^2\rangle B_{NS} = 0.30,$$

for a χ^2/d.o.f. $= \frac{195}{120-5}$.

Clearly, the best fit is obtained with the hard plus soft Pomerons. Not only the $\chi^2/\text{d.o.f.}$ is quite good, but the values of the parameters are very reasonable. In fact, more evidence in favour of the "hard plus soft" scenario will be given in next section; for now we will consider that the fits are so good, that it makes sense to see if one can find evidence for a "triple Pomeron" term. That is, we consider that [cf. Eq. (5.1)]

$$F_S = F_{\text{Soft}} + F_{\text{Hard}} + F^{TP},$$
$$F^{TP}(x,Q_0^2) \simeq (\text{Const.})\, x^{-2\lambda},$$

so that, when evolved with QCD to large Q^2,

$$F^{TP}(x,Q^2) \simeq B_{TP}\left\{1+\frac{c_S(1+2\lambda)\alpha_s}{4\pi}\right\} \mathrm{e}^{q_S(1+2\lambda)\alpha_s/4\pi}[\alpha_s(Q^2)]^{-d_+(1+2\lambda)}x^{-2\lambda}. \tag{5.6}$$

Note that this is $O(\alpha_s^{d_+(1+\lambda)-d_+(1+2\lambda)}) \simeq O(\alpha_s^{1.4})$, i.e., subleading in powers of α_s, with respect to F_{Hard}.

We present in Table X the parameters of the fits to, simultaneously, H1 and Zeus data on ep, plus neutrino data. This gives our best set of formulas, providing an excellent fit to experiment in a very wide range of Q^2, x. In the second case (Table Xb) we do not give the fit including a triple Pomeron term as the $\chi^2/\text{d.o.f.}$ does not vary appreciably if including it provided $\langle e_q^2\rangle|B_{TP}| \lesssim 2\times 10^{-4}$. We consider the parameters given in Table Xa and Table Xc (see below) to be the more reliable ones for describing small x structure functions. If we had fitted also λ with the whole set of data we would have obtained minima for values comprised between 0.42 and 0.49, with a variation of the chi-squared of less than two units with respect to the one obtained fixing $\lambda = 0.470$. Finally, if we fit the QCD parameter Λ, the values which provide minima vary between 0.555 GeV and 0.310 GeV, and the chi-squared improves by less than five units. Because of this we consider, as stated, that it is justified to favour the fits obtained with *fixed* $\lambda = 0.470$, $\Lambda = 0.23\,\text{GeV}$.

Table Xa. $n_f = 4$; Zeus plus H1 data; $Q^2 \geq 10\,\text{GeV}^2$, $x \leq 0.01$.

	λ (fixed)	Q_0^2	$\langle e_q^2\rangle c_P$	$\langle e_q^2\rangle B_S$	$\langle e_q^2\rangle B_{NS}$	$\chi^2/\text{d.o.f.}$
Hard + P	0.47	$2.95\,\text{GeV}^2$	0.296	4.28×10^{-4}	0.349	$\frac{138.3}{144-4}$

	λ (fixed)	Q_0^2	$\langle e_q^2\rangle c_P$	$\langle e_q^2\rangle B_S$	$\langle e_q^2\rangle B_{TP}$	$\langle e_q^2\rangle B_{NS}$	$\chi^2/\text{d.o.f.}$
Hard + P, +TP term	0.47	$4.45\,\text{GeV}^2$	0.258	8.33×10^{-4}	-1.67×10^{-4}	0.359	$\frac{129.3}{144-5}$

Table Xb. $n_f = 4$; Zeus plus H1 data; $Q^2 \geq 10\,\text{GeV}^2$, $x \leq 0.032$.

	λ (fixed)	Q_0^2	$\langle e_q^2\rangle c_P$	$\langle e_q^2\rangle B_S$	$\langle e_q^2\rangle B_{NS}$	$\chi^2/\text{d.o.f.}$
Hard + P x "softened" with $(1-x)^\nu$	0.47	$2.28\,\text{GeV}^2$	0.311	2.72×10^{-4}	0.315	$\frac{227.4}{230-4}$

Table Xc. $n_f = 4$; Zeus plus H1 data; $Q^2 \geq 10\,\text{GeV}^2$, $x \leq 0.032$..

	λ (fixed)	Q_0^2	$\langle e_q^2\rangle c_P$	$\langle e_q^2\rangle C_{P'}$	$\langle e_q^2\rangle B_S$	$\langle e_q^2\rangle B_{NS}$	$\chi^2/\text{d.o.f.}$
Hard + P + P'	0.47	$5.00\,\text{GeV}^2$	0.588	-0.271	4.66×10^{-4}	0.262	$\frac{265.3}{230-5}$

Λ fixed at 0.230 GeV. NLO corrections included

We discuss now in some detail the larger x region. If taken by themselves, both soft and hard Pomeron expressions (and *a fortiori* a sum of the two) must, as discussed in ref. 1 and Sect. 3.1 here, run in contradiction with the momentum sum rule if mantained for fixed x and $Q^2 \to \infty$; and this contradiction starts becoming noticeable at the higher $Q^2 \sim 1\,000\,\text{GeV}^2$ for $x \geq 0.02$: so a modification of our formulas for finite x is necessary. In the present paper we have, until now, introduced it phenomenologically by multiplying the low x expressions by a factor $(1-x)^\nu$

("softening"), with ν constant or depending on Q^2. A more rigorous procedure would be to assume, at a *fixed* Q_0^2, a behaviour like

$$F_S(x,Q_0^2) = (\bar{B}_S x^{-\lambda} + C)(1-x)^{\nu_0}, \tag{5.7}$$

and then evolve with QCD. This is best done by expanding first (5.7) in x,

$$F_S(x,Q_0^2) \simeq \bar{B}_S x^{-\lambda} + C - \nu_0 B_S x^{1-\lambda} + \ldots. \tag{5.8}$$

The dots correspond to terms behaving, as $x \to 0$, as higher powers of x, which need not be considered; see below. (5.8) has exactly the form of a hard Pomeron, plus a soft Pomeron, plus a P' Regge pole, plus higher powers of x. From the results of the previous sections we know that all terms vanishing for small x yield the same expression, *up to a constant*, when evolved to large Q^2, as the P' piece. So we may lump the piece $-\nu_0 B_S x^{1-\lambda} + \ldots$ into a single term like that of Eq. (5.5b), to be added to a soft and a hard term. To LO thus,

$$F_S(x,Q^2) \underset{\substack{x\to 0\\ Q^2\to\infty}}{\simeq} B_S \alpha_s^{-d_+} + F^P_{\rm corr.}(x,Q^2) + F^{P'}_{\rm corr.}(x,Q^2) \tag{5.9}$$

$F^P_{\rm corr.}(x,Q^2)$, $F^{P'}_{\rm corr.}(x,Q^2)$ given in Eqs. (5.5). The resulting fit (including NLO corrections) is described in Table Xc above. This certainly improves the fit at large x with respect to the unsoftened situation, but not much; indeed, less than the simple "softening" used before in the text[15], and it certainly does not solve the momentum sum rule problem, either. This should not be too surprising: by its very nature, a calculation with leading terms only for x must fail for larger values of this variable.

What we mean by this exactly is the following. Consider that at a fixed Q_0^2 one had exactly a hard Pomeron, $F_S(x,Q_0^2) = \bar{B}x^{-\lambda}$. Then, at any larger Q^2, we have the moments [in this simplified discussion we neglect the matrix character of the evolution equations]

$$\mu(n,Q^2) = \bar{B}\left[\frac{\alpha_s(Q_0^2)}{\alpha_s(Q^2)}\right]^{d_+(n)} \frac{1}{n-(1+\lambda)}.$$

Writing identically $\mathrm{e}^{\tau d_+(n)} \equiv \mathrm{e}^{\tau d_+(1+\lambda)}[1+\delta(n,\lambda)]$ we find

$$F_S(x,Q^2) = F_S^{\rm Lead.} + F_S^{\rm SL};\ F_S^{\rm Lead.}(x,Q^2) = B_S[\alpha_s(Q^2)]^{-d_+(1+\lambda)} x^{-\lambda},$$

and the subleading piece is such that it has moments

$$\mu^{\rm SL}(n,Q^2) = B_S[\alpha_s(Q^2)]^{-d_+(1+\lambda)} \frac{\delta(n,\lambda)}{n-(1+\lambda)}.$$

$\delta(n,\lambda)$ vanishes for $n = 1+\lambda$; hence the first singularity of the $\mu^{\rm SL}(n,Q^2)$ occurs for $n=1$ and there,

$$\mu^{\rm SL}(n,Q^2) \underset{n\to 1}{\simeq} \frac{-B_S}{1+\lambda}\alpha_s^{-d_+(1+\lambda)} \exp\tau\left[\frac{d_0}{4(n-1)} - d_1\right].$$

This is of the soft-Pomeron type apart from the factor $\alpha_s^{-d_+(1+\lambda)}$, so we expect

$$F_S^{\rm SL}(x,Q^2) \sim \alpha_s^{-d_+(1+\lambda)+d_1} \mathrm{e}^{\sqrt{d_0\tau\xi}}.$$

If we continie to subtract the tems singular at $n = 1, 2, \ldots$, we would get an asymptotic series for F_S. For $x \to 0$ this is dominated by the term $F_S^{\rm Lead.}$; but for fixed x, the remaining terms in the series end up by overwhelming $F_S^{\rm Lead.}$ as Q^2 becomes *very* large.

A precise evaluation is not difficult; it would also involve the gluon component. We shall not present the corresponding fits here; to do so one would have to include also subdominant corrections to the *soft* Pomeron piece. It is unclear that the effort would be worth the results, given the good quality of the fits with dominant terms only.

[15] Nevertheless, from the point of view of *rigorous* QCD the softening given in Eq. (5.9) is to be preferred to mere multiplication by $(1-x)^\nu$ for all Q^2; e.g., for extrapolations to higher Q^2, since (5.9) is compatible with QCD evolution for $x \to 0$. What is more, the parameters are fairly stable from Table Xa ot Table Xc, advantages that in our opinion offset a small increase in χ^2/d.o.f.. wit respect to Table Xb.

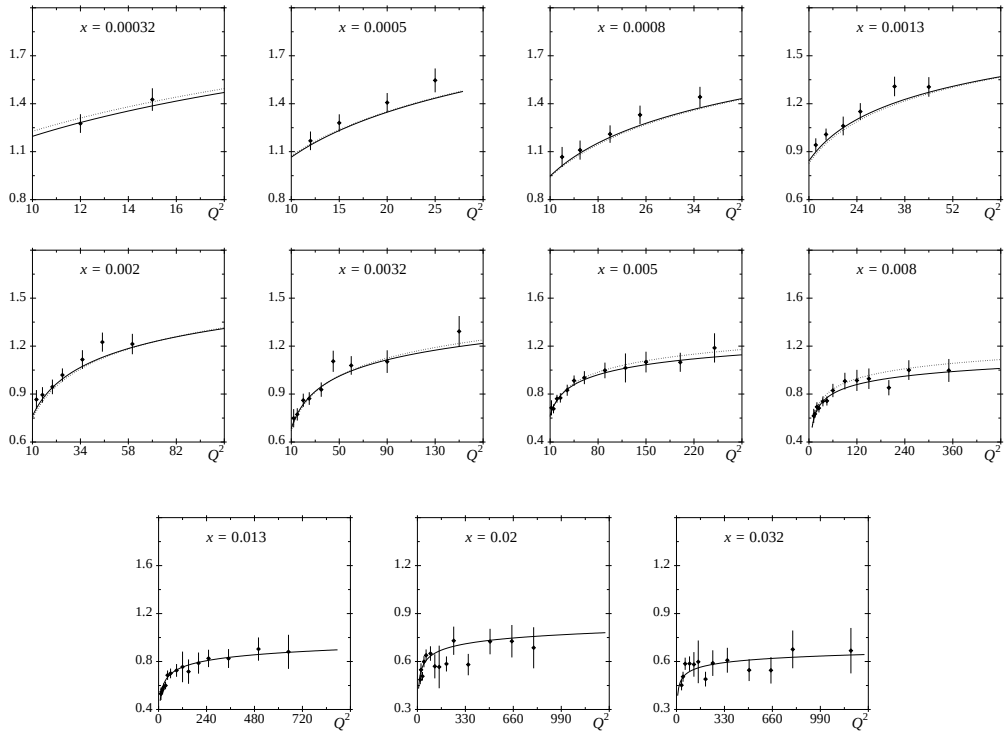

Figure 8a. Comparison of predictions from Table X with H1 ep data for F_2.

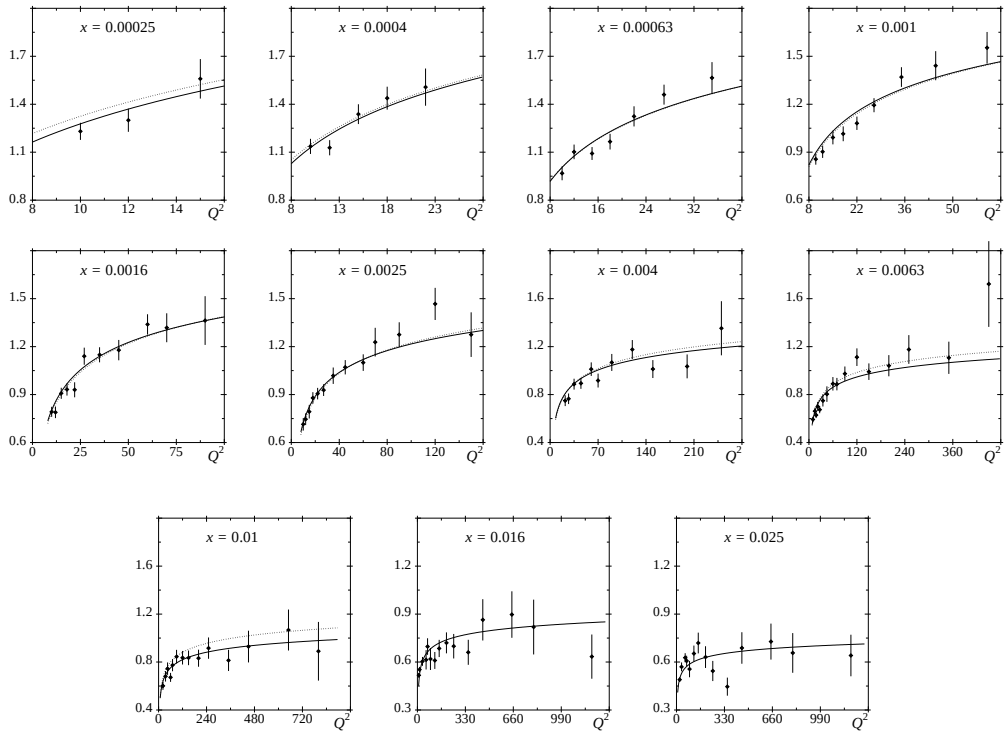

Figure 8b. Comparison of predictions from Table X with Zeus ep data for F_2.

In Figs. 8 we show the comparison of our fits, with the parameters in Table X, with data. Note that the *same* values of the parameters are used in Fig. 8a and Fig. 8b. For both Figs. 8 we give the fits with the "softened" and straight formulas: the continuous lines indicate large-x softening, and the dotted lines no softening. The improvement in the quality of the fits when compared with the "soft-Pomeron only" or "hard-Pomeron only" is obvious to the naked eye here.

5.3. Gluon and longitudinal structure functions.

Detailed predictions for the gluon and longitudinal structure functions are obtained trivially by adding the soft and hard Pomeron expressions given in the previous sections We will leave the details of this to the reader; likewise, we do not draw the figures for the F_G, F_L as they would not differ much from the ones drawn for, say, the hard Pomeron-only hypothesis. However we would like to comment here on a particularly interesting prediction of our analysis for the growth of the cross-section $\sigma_{\gamma p\to J/\psi p}(W)$ as a function of the c.m. energy, W. In fact, this cross section may be expressed as a function of the gluon structure function F_G,

$$\sigma_{\gamma p\to J/\psi p}(W) = AF_G(\bar{x} = a\frac{M^2_{J/\psi}}{W^2}, Q^2 = M^2_{J/\psi}) \simeq 9\,\mathrm{GeV}^2,$$

and A, a are constants approximately known. For F_G we have,

$$F_G(x,Q^2) \underset{x\to 0}{\simeq} B_G[\alpha_s]^{-d_+}x^{-\lambda}$$

and B_G may be calculated in terms of λ, B_S. So, using our formulas we have, for the logarithmic *slope* of the cross section,

$$\delta \equiv \frac{\log\sigma_{\gamma p\to J/\psi p}(W)}{\log W} \underset{s\to\infty}{\to} 2\lambda.$$

The figure reported in a fit[26] including recent HERA data[27] gives $\delta = 2\lambda = 0.9$. This in very good agreement with the optimum values of λ obtained with the hard plus soft fits, $2\lambda = 0.83$ to 1.0, and is clearly superior to the results following from the hard Pomeron only hypothesis, $2\lambda = 0.64$ to 0.76.

6. HARD PLUS SOFT SINGULARITIES: SMALL Q^2.

The quality of the results obtained by assuming that at values of $Q_0^2 \sim 3\,\mathrm{GeV}^2$ one has a hard singularity, $x^{-\lambda}$, plus a soft (constant) Pomeron term, evolved with QCD to large values $Q^2 \geq 10\,\mathrm{GeV}^2$, leads us naturally to the question wether it is possible to extend the analysis to the *low* Q^2 region as well, thus enabling us to address the important issue of the connection between the perturbative regime ($Q^2 \geq 10\,\mathrm{GeV}^2$, say) and the region $Q^2 < 10\,\mathrm{GeV}^2$ where nonperturbative effects are determinant.

It should be obvious that, unless one were able to perform a full, nonperturbative calculation, we must content ourselves with *phenomenological* evaluations. Here we use approximate, QCD-inspired formulas and assumptions and enquire wether we can still fit the data. We will find that this is indeed the case; in particular, we will see that the extension of the fit of the data to $Q^2 \to 0$ implies self-consistency conditions both for the singlet and the nonsinglet which will allow us to *calculate* the constants λ, ρ, getting values in impressive agreement with other (in particular, high Q^2) determinations.

The expression for the virtual photon scattering cross section in terms of the structure function F_2 is

$$\sigma_{\gamma(Q^2=0)p}(s) = \frac{4\pi\alpha}{Q^2}F_2(x,Q^2), \text{ with } s = Q^2/x. \tag{6.1}$$

We would like to describe this down to $Q^2 \to 0$. In the low energy region we should, as discussed, take the soft-Pomeron dominated expression to be given by an ordinary Pomeron, i.e. , behaving as a constant for $x \to 0$ (or equivalently, $s \to \infty$): the expression for F_2 that will, when evolved to large Q^2 yield (5.4), (5.5a) is

$$\begin{aligned} F_2 = \langle e_q^2\rangle\Big\{ & B_S[\alpha_s(Q^2)]^{-d_+(1+\lambda_0)}x^{-\lambda_0} \\ & + C + B_{NS}[\alpha_s(Q^2)]^{-d_{NS}(1-\rho_0)}x^{\rho_0}\Big\}. \end{aligned} \tag{6.2}$$

Because NLO corrections are large for $Q^2 \leq 10\,\mathrm{GeV}^2$ and we are interested in a semi-phenomenological description, only LO formulas will be used. Note also that the C in Eq. (6.2) is different from the c_0 in, say, (1.4a) as the gluon component also intervenes in the evolution.

On comparing (6.1) and (6.2) we see that, as noted in ref. 1, we have problems if we want to extend (6.2) to very small Q^2. First of all,

$$\alpha_s(Q^2) = \frac{4\pi}{\beta_0 \log Q^2/\Lambda^2} \tag{6.3}$$

diverges when $Q^2 \sim \Lambda^2$. Secondly, Eq. (6.1) contains the factor Q^2 in the denominator so the cross section blows up as $Q^2 \to 0$ unless F_2 were to develop a zero there.

It turns out that there is a simple way to solve both difficulties at the same time. It has been conjectured[28] that the expression (6.3) for α_s should be modified for values of Q^2 near Λ^2 in such a way that it *saturates*, producing in particular a finite value for $Q^2 \sim \Lambda^2$. To be precise, one alters (6.3) according to

$$\alpha_s(Q^2) \to \frac{4\pi}{\beta_0 \log(Q^2 + M^2)/\Lambda^2},$$

where M is a typical hadronic mass, $M \sim m_\rho \sim \Lambda(n_f = 2)\ldots$; the value $M = 0.96\,\mathrm{GeV}$ has been suggested on the basis of lattice calculations. It has been argued that saturation incorporates important nonperturbative effects. In the present paper we will simply set $M = \Lambda = \Lambda_{\mathrm{eff}}$, to avoid a proliferation of parameters. For the Pomeron term [the constant in Eq. (6.2)] we merely replace $C \to Q^2/(Q^2 + \Lambda^2_{\mathrm{eff}})$, using a procedure similar to that of ref. 29. The expression we will use for low Q^2 is thus,

$$\begin{aligned} F_2 = \langle e_q^2 \rangle \Big\{ & B_S [\tilde{\alpha}_s(Q^2)]^{-d_+(1+\lambda)} Q^{-2\lambda} s^\lambda \\ + C \frac{Q^2}{Q^2 + \Lambda^2_{\mathrm{eff}}} & + B_{NS} [\tilde{\alpha}_s(Q^2)]^{-d_{NS}(1-\rho)} Q^{2\rho} s^{-\rho} \Big\}, \end{aligned} \tag{6.4a}$$

where

$$\tilde{\alpha}_s(Q^2) = \frac{4\pi}{\beta_0 \log(Q^2 + \Lambda^2_{\mathrm{eff}})/\Lambda^2_{\mathrm{eff}}} \tag{6.4b}$$

and we have changed variables, $(Q^2,\, x) \to (Q^2,\, s = Q^2/x)$.

We have still not solved our problems: given Eq. (6.1) it is clear that a *finite* cross section for $Q^2 \to 0$ will only be obtained if the powers of Q^2 match exactly. This is automatic by construction for the Pomeron term, but for the hard singlet and the nonsinglet piece it will only occur if we have consistency conditions satisfied. With the expression given in (6.4b) for $\tilde{\alpha}_s$ it diverges as $\mathrm{Const.}/Q^2$ when $Q^2 \to 0$: so we only get a matching of zeros and divergences for $\sigma_{\gamma(Q^2=0)p}(s)$ if $\lambda = \lambda_0$, $\rho = \rho_0$ such that

$$d_+(1 + \lambda_0) = 1 + \lambda_0,\ d_{NS}(1 - \rho_0) = 1 - \rho_0\,. \tag{6.5}$$

The solution to these expressions depends very little on the number of flavours; for $n_f = 2$, probably the best choice at the values of Q^2 we will be working with, one finds $\lambda_0 = 0.470$, $\rho_0 = 0.522$. The second is in uncanny agreement with the value obtained with either a Regge analysis in hadron scattering processes, or by fitting structure functions in DIS. The first is larger than the value obtained in the fits to DIS with *only* a hard Pomeron, which gave $\lambda = 0.32$ to 0.38; but falls in the right ballpark of values obtained in the previous section with hard plus soft Pomeron, $\lambda = 0.43$ to 0.5.

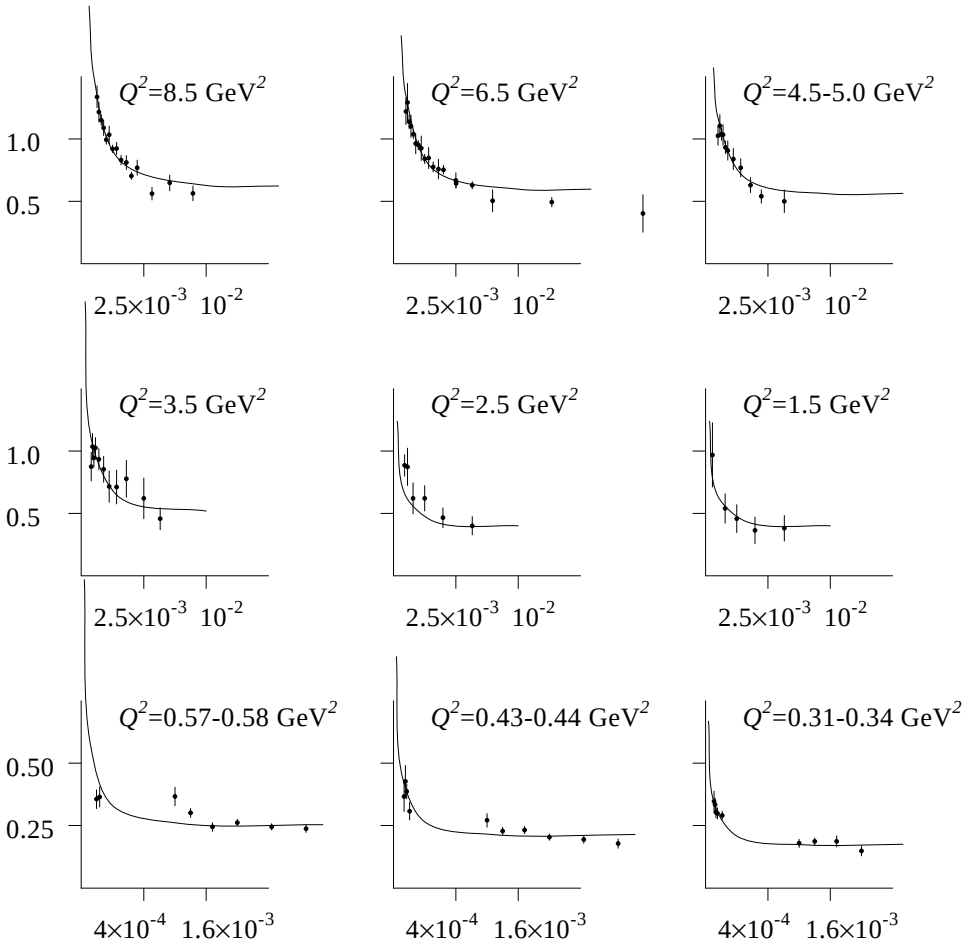

Figure 9. Comparison of predictions with data, Zeus plus H1. The neutrino data and prediction are not shown. We plot F_2 *vs.* $x^{1/2}$.

We are perfectly aware that, by using Eqs. (6.4) down to $Q^2 = 0.32\,\mathrm{GeV}^2$ we are pushing perturbative QCD well below its region of applicability, and that the condition of matching at $Q^2 \to 0$ is at best only of phenomenological value. Nevertheless, the fact that we get such reasonable predictions for λ_0, ρ_0 probably indicates that our procedure represents, *grosso modo*, the actual situation, which is also justified by the quality of the fit Eq. (6.4) provides. If we take all H1 and Zeus data for $0.31\,\mathrm{GeV}^2 \leq Q^2 \leq 8.5\,\mathrm{GeV}^2$, and we include also 10 neutrino xF_3 data we find

$$\Lambda_{\mathrm{eff}} = 0.87\,\mathrm{GeV},\ \langle e_q^2\rangle B_S = 5.28\times 10^{-3},\ \langle e_q^2\rangle B_{NS} = 0.498,\ \langle e_q^2\rangle C = 0.486,$$

for a $\chi^2/\mathrm{d.o.f.} = \frac{106.2}{104-4}$. The value of Λ_{eff} we have obtained lies somewhere inside the expected bracket, $\Lambda(n_f = 2) \simeq 0.35\,\mathrm{GeV}$ and the value found in the quoted lattice calculation for M, 0.96 GeV. Clearly, the fit gives a compromise, phenomenological quantity.

The agreement between phenomenology and experiment, shown graphically in Fig. 9, is unlikely to be trivial; x varies between 6×10^{-6} and 4×10^{-2} , and F_2 changes by almost one order of magnitude. To see more clearly this nontriviality, we replace the hard singularity by an evolved soft Pomeron, with a saturated α_s. That is, we now fit with the expression

$$F_2 = \langle e_q^2\rangle\Bigg\{\frac{c_0}{\xi}\left[\frac{9\xi\log[\tilde\alpha_s(Q_0^2)/\tilde\alpha_s(Q^2)]}{4\pi^2(33-2n_f)}\right]^{\frac{1}{4}}\exp\left(\sqrt{d_0\xi\,\left[\log\frac{\tilde\alpha_s(Q_0^2)}{\tilde\alpha_s(Q^2)}\right]}-d_1\log\frac{\tilde\alpha_s(Q_0^2)}{\tilde\alpha_s(Q^2)}\right)$$
$$+C\frac{Q^2}{Q^2+\Lambda_{\rm eff}^2}+B_{NS}[\tilde\alpha_s(Q^2)]^{-d_{NS}(1-\rho)}Q^{2\rho}s^{-\rho}\Bigg\},$$

$\tilde\alpha_s$ as before. Then we find

$$\Lambda_{\rm eff}=0.41\,{\rm GeV},\ \langle e_q^2\rangle c_0=0.094,\ \langle e_q^2\rangle C=0.253,\ \langle e_q^2\rangle B_{NS}=0.41$$

and a much deteriorated $\chi^2/{\rm d.o.f.}=250/(104-4)$. We consider these results as convincing proof of the necessity of a hard component also at low Q^2.

7. DISCUSSION

The main outcome of our analysis in the present paper is that we are able to give a unified, consistent description of small x DIS data, both for large and small values of Q^2, by assuming, at low momenta, the presence of a hard plus a soft Pomeron, a procedure which improves substantially the quality of the descriptions with only one of these. There also appears some evidence for a triple Pomeron contribution; evidence which is, however, somewhat marginal. Besides this, there are a number of specific points to which we would like to draw also attention.

First of all there is the matter of the dependence of our low Q^2 results on the saturation hypothesis for α_s. It is clear that the good quality of the fits indicates that, with suitable modifications, perturbative QCD supplemented by saturation, may give a *phenomenological* description of the data down to very low momenta; but of course this should not be construed as a proof of saturation, in particular of the very specific form considered here. One may interpret our results, however, as showing that the saturation expression is particularly adapted to represent, in DIS, a variety of effects: higher twists, renormalons, and likely also genuine saturation.

A second question is the connection between low and high Q^2. For the hard piece there is no problem, as both expressions are identical up to NLO corrections. For the soft piece, if we start with a constant behaviour for $Q^2\sim 2-5\,{\rm GeV}^2$, then as Q^2 grows an expression like (2) will start to develop. the details of this will depend on what one assumes for the gluon structure function. Because the variation both with Q^2 and x of the soft piece is slower than that of the hard part, we think the best procedure is to assume constancy of the soft piece up to $Q^2=8.5\,{\rm GeV}^2$, and the evolved form from there on; since a very good fit is obtained at the low momentum region already with the constant behaviour there is little point in adding frills, and a new constant (the soft component of the gluon structure function).

Next, we say a few words on the parameters, starting with the QCD parameter, Λ. It is impossible to give a reliable determination of the value of this parameter from low x data alone; if fitting it, the central values vary between $0.08\,{\rm GeV}$ and $0.55\,{\rm GeV}$. If we take what we consider the more reliable fits, those in Tables Xa, c, and allow Λ to vary, we find an optimum value of $0.31\,{\rm GeV}$; in particular, from the fit with hard plus soft Pomerons, plus P', the optimum is $\Lambda=0.32\pm0.05$ MeV for a $\chi^2/{\rm d.o.f.}$ of $\frac{261}{230-6}$, hardly improving the result reported in Table Xc. This tells us little more than rough compatibility between the low x and other determinations of Λ.

With respect to other parameters, we can say that the fits give precise determinations of the *nonsinglet* parameters, ρ, B_{NS}; but the singlet parameters are much less precisely determined. For example, λ varies from 0.38 (LO, hard singularity only) to 0.32 (NLO, hard singularity only) to 0.47 ± 0.04 (hard plus soft, the best value in our opinion). Likewise, B_S varies by almost one order of magnitude. The reason for this may be traced to the dependence of the parameters on the theoretical formulas used to fit the data, in particular when going from LO to NLO because of the large size of the NLO corrections to F_S. We consider the parameters given in Tables Xa, c to be the more reliable ones in particular for extrapolations to larger Q^2.

APPENDIX

In this Appendix we present the full collection of formulas necessary to evaluate electroproduction to NLO.

Leading order quantities.

$\beta_0 = 11 - \frac{2}{3}n_f$, $\beta_1 = 102 - \frac{38}{3}n_f$.

$$d_{NS}(n) = -\frac{\gamma_{NS}^{(0)}(n)}{2\beta_0};\ \mathbf{D}(n) = -\frac{\boldsymbol{\gamma}^{(0)}(n)}{2\beta_0}. \tag{A.1}$$

Here, $\gamma_{NS}^{(0)}(n) = \gamma_{11}^{(0)}(n)$ and

$$\boldsymbol{\gamma}^{(0)} = -\frac{32}{3}\begin{pmatrix} \dfrac{1}{2n(n+1)} + \frac{3}{4} - S_1(n) & \frac{3}{8}n_f\,\dfrac{n^2+n+2}{n(n+1)(n+2)} \\ \dfrac{n^2+n+2}{2n(n^2-1)} & \dfrac{33-2n_f}{16} + \frac{9}{4}\left[\dfrac{1}{n(n-1)} + \dfrac{1}{(n+1)(n+2)} - S_1(n)\right] \end{pmatrix} \tag{A.2}$$

We define, generally, the functions

$$S_l(n) = \sum_{k=1}^{\infty}\left[\frac{1}{k^l} - \frac{1}{(k+n)^l}\right],\ S_l^+(\tfrac{1}{2}n) = S_l(n/2);\ S_l^-(\tfrac{1}{2}n) = S_l\left(\frac{n-1}{2}\right),$$

and

$$\tilde{S}^{\pm}(n) = -\tfrac{5}{8}\zeta(3) \mp \sum_{k=1}^{\infty}\frac{(-1)^k}{(k+n)^2}\,S_1(k+n).$$

The matrix that diagonalizes $\mathbf{D}(n)$ is $\mathbf{S}(n)$,

$$\mathbf{S}(n)^{-1}\mathbf{D}(n)\mathbf{S}(n) = \begin{pmatrix} d_+(n) & 0 \\ 0 & d_-(n) \end{pmatrix},$$

with the eigenvalues ordered so that $d_+ > d_-$. $\mathbf{S}$ may be written as

$$\mathbf{S}(n) = \begin{pmatrix} 1 & \dfrac{D_{12}(n)}{d_-(n) - d_+(n)} \\ \dfrac{d_+(n) - D_{11}(n)}{D_{12}(n)} & \dfrac{d_-(n) - D_{11}(n)}{d_-(n) - d_+(n)} \end{pmatrix}. \tag{A.3}$$

Nonsinglet NLO quantities.

We will not give explicit formulas for the $C_{NS}^{(1)}(n)$, $\gamma_{NS}^{(1)}(n)$, which may be found, misprint free, in refs. 6, 7. We will only present a few figures for relevant values of n from which good interpolation formulas may be written. One has

$$C_{NS}^{(1)}(n=1) = 0;\ \gamma_{NS}^{(1)}(1) = \tfrac{8}{9}[13 + 8\zeta(3) - 2\pi^2],$$

the last formula for crossing-even functions (like F_{NS} in electroproduction). For crossing odd functions, like xF_3 in neutrino scattering, the corresponding NLO anomalous dimension coefficient verifies

$$\gamma_{NS,\mathrm{odd}}^{(1)}(1) = 0.$$

For n near 0.5,

$C_{NS}^{(1)}(n) =$	$n=0.4$	$n=0.5$	$n=0.6$						
	17.1;	9.6;	5.5						
	$n_f=3$			$n_f=4$			$n_f=5$		
$n=$	0.4	0.5	0.6;	0.4	0.5	0.6;	0.4	0.5	0.6
$\gamma_{NS}^{(1)} =$	−273.7	−159.3	−98.2;	−271.7	−155.9	−95.0;	−269.6	−152.5	−91.7

Note that $C_{NS}^{(1)}(n)$ is independent of n_f.

Singlet NLO quantities.

The four quantities $C_{ij}(n)$ may be found in ref. 6. Here we give only the two that enter the calculation for ep scattering. With $C_F = 4/3, C_A = 3, T_F = 1/2$,

$$C_{11}^{(1)}(n) = C_F\left\{2S_1^2(n) + 3S_1(n) - 2S_2(n) - \frac{2S_1(n)}{n(n+1)} - 9 + \frac{3}{n} + \frac{4}{n+1} + \frac{2}{n^2}\right\}; \tag{A.4a}$$

$$C_{12}^{(1)}(n) = 4n_f T_F \left\{ -\frac{1}{n} + \frac{1}{n^2} + \frac{6}{(n+1)(n+2)} - S_1(n)\,\frac{n^2+n+2}{n(n+1)(n+2)} \right\}. \tag{A.4b}$$

Finally, for the NLO anomalous dimension matrix $\boldsymbol{\gamma}^{(1)}(n)$ we have the following expressions:

$$\begin{aligned}
\gamma_{11}^{(1)}(n) = C_F^2 \Bigg\{ & 16 S_1(n)\,\frac{2n+1}{n^2(n+1)^2} + 16\left(2S_1(n) - \frac{1}{n(n+1)}\right)\left[S_2(n) - S_2^+(\tfrac{1}{2}n)\right] \\
& + 24 S_2(n) + 64\tilde{S}(n) - 8 S_3^+(\tfrac{1}{2}n) - 3 - 8\,\frac{3n^3+n^2-1}{n^3(n+1)^3} - 16\,\frac{2n^2+2n+1}{n^3(n+1)^3} \Bigg\} \\
& + C_F C_A \Bigg\{ \tfrac{536}{9} S_1(n) - 8\left(2S_1(n) - \frac{1}{n(n+1)}\right)\left[2S_2(n) - S_2^+(\tfrac{1}{2}n)\right] \\
& - \tfrac{88}{3} S_2(n) - 32\tilde{S}(n) + 4 S_3^+(\tfrac{1}{2}n) - \tfrac{17}{3} \\
& - \tfrac{4}{9}\,\frac{151n^4+236n^3+88n^2+3n+18}{n^3(n+1)^3} + 8\,\frac{2n^2+2n+1}{n^3(n+1)^3} \Bigg\} \\
& + n_f T_F C_F \Big\{ -\tfrac{160}{9} S_1(n) + \tfrac{32}{3} S_2(n) + \tfrac{4}{3} \\
& + \tfrac{16}{9}\,\frac{11n^7+49n^6+5n^5-329n^4-514n^3-350n^2-240n-72}{(n-1)n^3(n+1)^3(n+2)^2} \Bigg\};
\end{aligned} \tag{A.5a}$$

$$\begin{aligned}
-\gamma_{12}^{(1)}(n) = 8 n_f T_F C_A \Bigg\{ & \left[-2S_1^2(n) + 2S_2(n) - 2S_2^+(\tfrac{1}{2}n) \right] \frac{n^2+n+2}{n(n+1)(n+2)} \\
& + 8 S_1(n)\,\frac{2n+3}{(n+1)^2(n+2)^2} + \frac{3n^4+15n^3+29n^2+50n+44}{n(n+1)^3(n+2)^3} \\
& + \frac{2n^9+12n^8+27n^7+38n^6+58n^5+149n^4+262n^3+252n^2+128n+32}{(n-1)n^3(n+1)^3(n+2)^3} \Bigg\} \\
& + 8 n_f T_F C_F \Bigg\{ \left[2S_1^2(n) - 2S_2(n) + 5 \right] \frac{n^2+n+2}{n(n+1)(n+2)} - \frac{4S_1(n)}{n^2} \\
& + \frac{11n^4+26n^3+15n^2+8n+4}{n^3(n+1)^3(n+2)} \Bigg\}.
\end{aligned} \tag{A.5b}$$

This corrects a misprint in ref. 8 (a figure $262n^3$ instead of $26n^3$ in the third line).

$$\begin{aligned}
-\gamma_{21}^{(1)}(n) = 4 C_F^2 \Bigg\{ & \left[-2S_1^2(n) + 10 S_1(n) - 2S_2(n) \right] \frac{n^2+n+2}{(n^2-1)n} \\
& - \frac{4S_1(n)}{(n+1)^2} - \frac{12n^6+30n^5+43n^4+28n^3-n^2-12n-4}{(n-1)n^3(n+1)^3} \Bigg\} \\
& + 8 C_F C_A \Bigg\{ \left[S_1^2(n) + S_2(n) - S_2^+(\tfrac{1}{2}n) \right] \frac{n^2+n+2}{n(n^2-1)} \\
& - S_1(n)\,\frac{17n^4+41n^2-22n-12}{3(n-1)^2n^2(n+1)} + \frac{n^3+n^2+4n+2}{n^3(n+1)^3} \\
& + \frac{109n^8+512n^7+879n^6+772n^5-104n^4-954n^3-278n^2+288n+72}{9(n-1)^2n^3(n+1)^2(n+2)^2} \Bigg\} \\
& + \tfrac{32}{3} n_f T_F C_F \left\{ \left[S_1(n) - \tfrac{8}{3} \right] \frac{n^2+n+2}{n(n^2-1)} + \frac{1}{(n+1)^2} \right\};
\end{aligned} \tag{A.5c}$$

$$\begin{aligned}
\gamma_{22}^{(1)}(n) = n_f T_F C_A \left\{ -\tfrac{160}{9} S_1(n) + \frac{32}{3} + \tfrac{16}{9} \frac{38n^4+76n^3+94n^2+56n+12}{(n-1)n^2(n+1)^2(n+2)} \right\} \\
+ n_f T_F C_F \left\{ 8 + 16 \frac{2n^6+4n^5+n^4-10n^3-5n^2-4n-4}{(n-1)n^3(n+1)^3(n+2)} \right\} \\
+ C_A^2 \left\{ -16 S_1(n) S_2(n) + 32 \tilde{S}(n) - 4 S_3^+(\tfrac{1}{2}n) \right. \\
+ 32 S_1(n) \left[\tfrac{67}{36} + \frac{1}{(n-1)^2} - \frac{1}{n^2} + \frac{1}{(n+1)^2} - \frac{1}{(n+2)^2} \right] \\
+ 16 S_2(n) \left[\frac{1}{n-1} - \frac{1}{n} + \frac{1}{n+1} - \frac{1}{n+2} \right] \\
+ 16 \left[S_2(n) - S_2^+(\tfrac{1}{2}n) \right] \left[S_1(n) - \frac{1}{n(n-1)} - \frac{1}{(n+1)(n+2)} \right] \\
- \tfrac{64}{3} - \frac{32}{n-1} - \frac{148}{9n(n+1)} + \frac{32}{n+2} - \frac{32}{(n-1)^2} \\
\left. - \frac{8}{3n^2} + \frac{88}{3(n+1)^2} - \frac{256}{3(n+2)^2} - \frac{32}{n^3} - \frac{32}{(n+1)^3} - \frac{64}{(n+2)^3} \right\}
\end{aligned} \tag{A.5d}$$

This last corrects two misprints of ref. 8, a factor $n_f T_F \equiv T_R$ instead of T_A in the first line, and a sign, $+1/(n+1)^2$ instead of $-1/(n+1)^2$ in the fourth line.

We finish by giving two values of the $C_{ij}^{(1)}$, $\gamma_{ij}^{(1)}$ and tables with a few listings, sufficient for the calculations we are interested in. As for the first, we have

$$C_{11}^{(1)}(2) = \tfrac{4}{9},\ C_{12}^{(1)}(2) = -\tfrac{1}{2} n_f\,,$$

$$\boldsymbol{\gamma}^{(1)}(2) = \tfrac{64}{243} \begin{pmatrix} 367 - 39 n_f & -\frac{1833}{32} n_f \\ -(367 - 39 n_f) & \frac{1833}{32} n_f \end{pmatrix}.$$

We give the tables for the quantities relevant for the exponential expression, q_S and c_S,

$$\begin{aligned}
F_S(x,Q^2) \underset{x\to 0}{\simeq} B_S \left\{ 1 + \frac{c_S (1+\lambda) \alpha_s(Q^2)}{4\pi} \right\} \\
\times \left[\alpha_s(Q^2) \right]^{-d_+(1+\lambda)} \mathrm{e}^{q_S (1+\lambda) \alpha_s(Q^2)/4\pi} x^{-\lambda},
\end{aligned}$$

with

$$c_S = C_{11}^{(1)} + \frac{(d_+ - D_{11}) C_{12}^{(1)}}{D_{12}},$$

$$q_S = \frac{\beta_1 d_+}{\beta_0} + \frac{\bar{\gamma}_{11}}{2\beta_0} + \frac{\bar{\gamma}_{21}}{2\beta_0 (d_- - d_+ + 1)} \frac{D_{12}}{d_- - d_+};$$

for the expanded expression just note that $w_S = q_S + c_S$. Then,

	$1+\lambda =$	1.20	1.275	1.3	1.325	1.35	1.375	1.42	1.47	1.50	1.94
$n_f = 3$	q_S	142.2	99.9	91.0	83.7	77.8	72.9	66.3	61.8	60.5	−5.7
$n_f = 4$	q_S	147.9	103.1	93.5	85.7	79.2	73.8	66.1	60.2	57.8	−13.8
$n_f = 5$	q_S	153.6	106.2	96.1	87.6	80.6	74.6	66.1	59.0	55.8	−82.0
$n_f = 3$	c_S	8.28	1.74	0.44	−0.59	−1.41	−2.07	−2.93	−3.53	−3.76	−2.61
$n_f = 4$	c_S	8.26	1.73	0.43	−0.59	−1.41	−2.06	−2.91	−3.50	−3.72	−2.59
$n_f = 5$	c_S	8.23	1.72	0.43	−0.59	−1.42	−2.05	−2.89	−3.47	−3.69	−2.57

For the gluon structure function,

$$F_G(x,Q^2) \underset{x\to 0}{\simeq} B_S \frac{d_+(1+\lambda) - D_{11}(1+\lambda)}{D_{12}(1+\lambda)}$$
$$\times \left\{1 + \frac{c_G(1+\lambda)\alpha_s(Q^2)}{4\pi}\right\} \left[\alpha_s(Q^2)\right]^{-d_+(1+\lambda)} \mathrm{e}^{q_G(1+\lambda)\alpha_s(Q^2)/4\pi} x^{-\lambda},$$

with

$$c_G \equiv c_S,$$
$$q_G = \frac{\beta_1 d_+}{\beta_0} + \frac{\bar\gamma_{11}}{2\beta_0} + \frac{\bar\gamma_{21}}{2\beta_0(d_- - d_+ + 1)} \frac{D_{12}}{d_- - d_+} \frac{d_- - D_{11}}{d_+ - D_{11}}.$$

One has,

	$1+\lambda =$	1.20	1.275	1.3	1.325	1.35	1.375	1.42	1.47	1.50	1.94
$n_f = 3$	q_G	37.59	20.43	16.77	13.74	11.17	8.96	5.65	2.61	0.96	
$n_f = 4$	q_G	42.49	23.04	18.87	15.39	12.44	9.89	6.06	2.56	0.69	
$n_f = 5$	q_G	47.36	25.60	20.91	16.99	13.65	10.77	6.44	2.51	0.43	

Coefficients and integrals for the longitudinal structure function.

We give the coefficient functions for ep scattering, with unified notation. With the definitions of Eqs. (2.12), and with the polylogarithm functions[16]

$$\mathrm{Li}_\nu(x) = \sum_{n=1}^{\infty} \frac{x^n}{n^\nu};\ L_{1,2}(x) = \tfrac{1}{2}\int_0^1 \mathrm{d}t\, \frac{\log^2(1-tx)}{t},$$

we have,

$$\begin{aligned} c_{NS}^{(1)L}(x) = 4C_F(C_A - 2C_F)\Big\{ & 4\frac{6-3x+47x^2-9x^3}{15x}\log x \\ & -4x\mathrm{Li}_2(-x)\big[\log x - 2\log(1+x)\big] \\ & -2x\log^2 x\log(1-x^2) + 4x\log x\log^2(1+x) - 4x\log x\,\mathrm{Li}_2(x) \\ & +2x(1-\tfrac{3}{5}x^2)\log^2 x - \frac{144+294x-1729x^2+216x^3}{90x} \\ & -4\frac{2+10x^2+5x^3-3x^5}{5x^2}\big[\mathrm{Li}_2(-x) + \log x\log(1+x)\big] \\ & +4x\zeta(2)\big[\log(1-x^2) - 1 + \tfrac{3}{5}x^2\big] - 8x\zeta(3) \\ & +8xL_{1,2}(-x) + 4x[\mathrm{Li}_3(x) + \mathrm{Li}_3(-x)] - \tfrac{23}{3}x\log(1-x)\Big\} \\ & +8C_F^2\Big\{ x\mathrm{Li}_2(x) + x\log^2\frac{x}{1-x} - 3x\zeta(2) \\ & -\big(1-\tfrac{22}{3}x\big)\log x + \big(1-\tfrac{25}{6}x\big)\log(1-x) - \frac{78-355x}{36}\Big\} \\ & -\tfrac{16}{3}n_f T_F C_F\Big\{ x\log\frac{x^2}{1-x} - 1 + \tfrac{25}{6}x\Big\}; \end{aligned} \tag{A.6a}$$

$$\begin{aligned} c_{PS}^{(1)L}(x) = \tfrac{32}{9}n_f T_F C_F\Big\{ & 3\frac{1-2x-2x^2}{x}(1-x)\log(1-x) - 9x(1-x) \\ & -\frac{(1-x)^3}{x} + 9x\big[\mathrm{Li}_2(x) + \log^2 x - \zeta(2)\big] + 9(1-x-2x^2)\log x\Big\}; \end{aligned} \tag{A.6b}$$

[16] $L_{1,2}$ denoted $S_{1,2}$ in refs. 12, 13.

$$
\begin{aligned}
c_G^{(1)L}(x) = 2n_f T_F C_F \Big\{ & (8+24x-32x^2)\log(1-x) \\
& +16x\big[\mathrm{Li}_2(1-x)+\log x\log(1-x)\big] \\
& +\left(-\tfrac{32}{3}x+\tfrac{64}{5}x^3+\tfrac{32}{15}x^{-2}\right)\big[\mathrm{Li}_2(-x)+\log x\log(1+x)\big] \\
& +\frac{\log x}{15}\left[-104-624x+288x^2-32x^{-1}\right]-32x\left(\tfrac{1}{3}+\tfrac{1}{5}x^2\right)\log^2 x \\
& +\left(-\tfrac{32}{3}x+\tfrac{64}{5}x^3\right)\zeta(2)-\tfrac{128}{15}-\tfrac{304}{5}x+\tfrac{336}{5}x^2+\tfrac{32}{15}x^{-1}\Big\} \qquad \text{(A.6c)} \\
+2n_f T_F C_A \Big\{ & -64x\mathrm{Li}_2(1-x)+32x(1+x)\big[\mathrm{Li}_2(-x)+\log x\log(1+x)\big] \\
& +16x(1-x)\log^2(1-x)+x(-96+32x)\log x\log(1-x)+48x\log^2 x \\
& +32x^2\zeta(2)+[16+128x-208x^2]\log x+\tfrac{16}{3}+\tfrac{272}{3}x-\tfrac{848}{9}x^2-\tfrac{16}{9}x^{-1} \\
& +\left[-16-144x+\tfrac{464}{3}x^2+\tfrac{16}{3}x^{-1}\right]\log(1-x)\Big\}.
\end{aligned}
$$

Integrals: for $n_f = 4$,

$\lambda =$	0	0.25	0.30	0.325	0.35	0.375	0.42	0.47	0.50
$I_{S1} =$	15.4	15.3	15.3	15.2	15.1	15.1	15.0	14.9	14.9
$I_{S2} =$	30.4	29.3	29.3	29.2	29.2	29.2	29.2	29.2	29.1
$I_{S3} =$	−7.11	−7.28	−7.28	−7.28	−7.27	−7.26	−7.25	−7.23	−7.21
$I_{PS} =$		−22.8	−20.1	−18.9	−17.8	−16.8	−15.3	−13.8	−13.0
$I_{G1} =$	−10.7	−11.4	−11.4	−11.3	−11.3	−11.2	−11.2	−11.0	−11.0
$I_{G2} =$		−2.42	0.30	1.46	2.52	3.48	4.99	6.41	7.14

(the values of the integrals not given when x-dependent).

ACKNOWLEDGEMENTS

We acknowledge interesting discussions with J. Terrón. One of us (FJY) is grateful to J. Sánchez-Guillén and G. Parente for information concerning the NLO corrections to the longitudinal structure functions, to A. B. Kaidalov for the relevance of multi-Regge analysis, and to M. McDermott for communicating the results of calculations which prompted the detailed study of the NLO predictions of the soft Pomeron model.

This work was partially supported by CICYT, Spain.

REFERENCES

1. F. J. Ynduráin,Preprint FTUAM 96-12 (revised), to be published in Proc. QCD 96, Nucl. Phys. Suppl.
2. F. Barreiro, C. López and F. J. Ynduráin, Z. Phys. C, **72** (1996) 561.
3.- M. Derrick et al, Z. Phys.C, **65** (1995) 397; Phys. Lett. **B345** (1995) 576.
4. H1 Collaboration, preprint DESY 96-039, 1996; Zeus Collaboration, preprint DESY 96-076, 1996.
5. C. López and F. J. Ynduráin, Nucl. Phys., **B171** (1980) 231 (LO).
6. C. López and F. J. Ynduráin, Nucl. Phys., **B183** (1981) 157 (NLO).
7. F. J. Ynduráin, *Quantum Chromodynamics*, Springer 1983; second edition as *The Theory of Quark and Gluon Interactions*, Springer. 1992
8. A. González-Arroyo, C. López and F. J. Ynduráin, Phys. Lett., **98B** (1981) 215.
9. A. De Rújula et al., Phys. Rev., **D10** (1974) 1649.
10. F. Martin, Phys. Rev., **D19** (1979) 1382.
11. R. D. Ball and S. Forte, Phys. Lett., **B358** (1995) 365 and CERN TH/95-323 (1995), to be published in Acta Phys. Polonica.
12. J. Sánchez-Guillén et al., Nucl. Phys., **B353** (1991) 337.
13. E. B. Zijstra and W. L. van Neerven , Phys. Lett., **B272** (1991) 476.
14. S. A. Larin and J. Vermaseren, Z. Phys. C, **57** (1993) 93.
15. E. Oltman et al., Z. Phys. C, **53** (1992) 51; P. Berge et al., Z. Phys. C, **49** (1991) 187; P. Z. Quintas et al., Phys. Rev. Lett., **71** (1993) 1307.
16. Particle Data Group, any issue.
17. M. Klein (H1 collaboration), 4th Int. Conf. on Deep inelastic Scattering, Rome, 1996.
18. H. L. Anderson et al., Phys. Rev., **D20** (1979) 2645; A. Bodek et al. *ibid*, 1471.
19. E. A. Kuraev, L. N. Lipatov and V. S. Fadin, Sov. Phys. JETP, **44** (1976) 443; Ya. Ya. Balitskii and L. N. Lipatov, Sov. J. Nucl. Phys., **28** (1978) 822.
20. M. Ciafalloni, Nucl. Phys. **B296** (1988) 49; S. Catani, F. Fiorini and G. Marchesini, Phys. Lett., **B234** (1990) 339 and Nucl. Phys. **B336** (1990) 18; S. Catani and F. Hautmann, Nucl. Phys., **B427** (1994) 475; J. Blümlein and A. Vogt, Acta Phys. Polonica, **B27** (1996), 1309.
21. A. De Roeck, M. Klein and Th. Naumann, DESY 96-063 (1996).
22. C. López and F. J. Ynduráin, Phys. Rev. Lett., **44** (1980) 1118.
23. E. Witten, Nucl. Phys., **B119** (1977) 189.
24. A. B. Kaidalov, Survey in High Energy Physics, Vol. 9 (1996) 143.
25. V. D. Barger and D. B. Cline, *Phenomenological Theories of High Energy Scattering*, Benjamin, 1969.
26. H. Klein, DESY 96-218 (1996).
27. M. Derrick et al., Phys. Lett., **B350** (1995) 134, and work quoted there.
28. Yu. A. Simonov, Yadernaya Fizika, **58** (1995) 113, and work quoted there.
29. B. Badelek and J. Kwiecinski, Phys. Lett. **B295** (1992) 263; Rev. Mod. Phys., **68** (1996) 445.